Probing new physics using $t\bar{t}$ spin measurements at CMS

Jacob Linacre
(RAL)

9th May 2018

This project has received funding from the European Union's Horizon 2020 research and innovation programme under the Marie Skłodowska-Curie grant agreement (GA) No. 752730

Outline

- Introduction
- Top quark polarisation and spin correlations in the SM
- Leptonic angular distributions
- Correcting the reconstructed data
- Differential cross sections
- Interpretations

What's special about the top quark?

- **By far the heaviest quark ($m_t \sim 172$ GeV)**
  - elementary particle with mass of a gold atom!
  - strong Yukawa coupling to the Higgs
    → is there an underlying reason?
    - if NP stabilises EW scale, BSM likely to be top-phlic

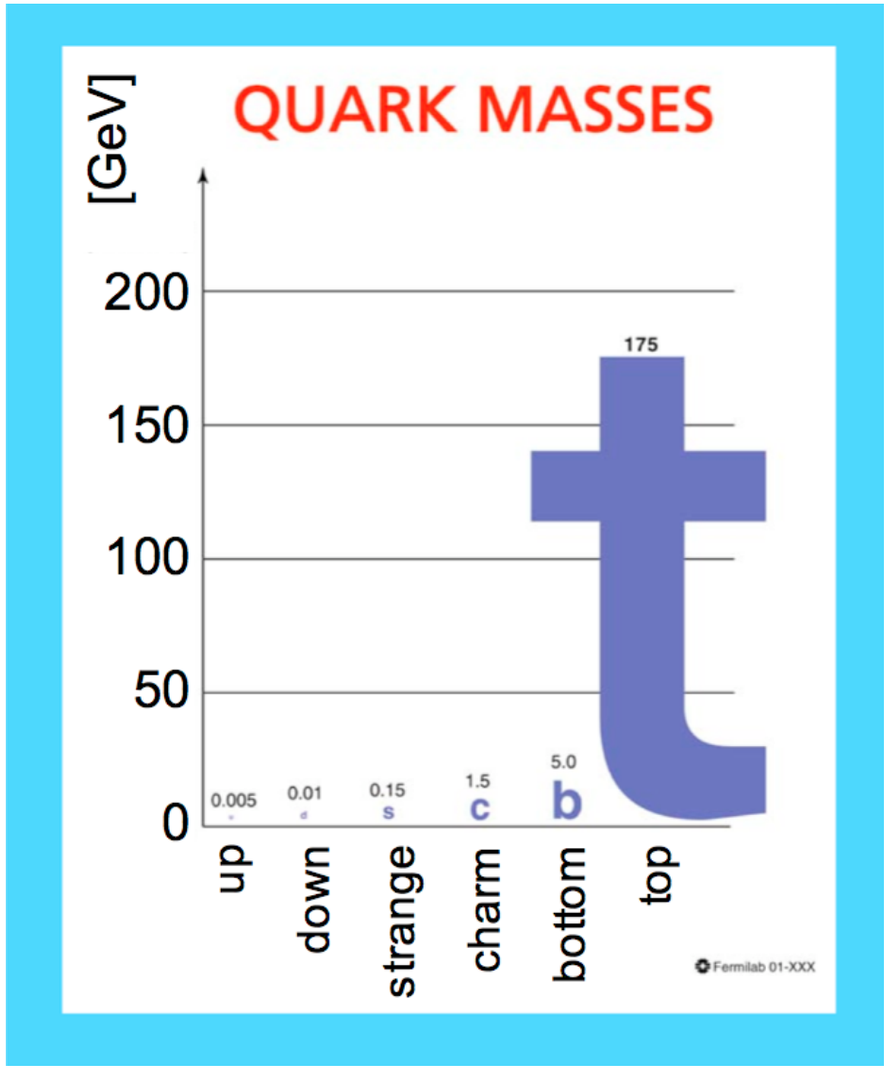

- **Top decays before it can form bound states**
  - unique opportunity to study a "bare" quark, free from effects of colour confinement
  - spin information **transferred to daughter particles**
  - expect top spin variables to be **well predicted by perturbative QCD**

$$\text{lifetime} < \text{QCD timescale} \ll \text{spin-flip timescale}$$

$$10^{-25}\,\text{s} < 10^{-24}\,\text{s} \ll 10^{-21}\,\text{s}$$

Spin properties

- Spin measurements in top events provide **excellent laboratory to probe new physics**
  - new mediator?
  - new particles decaying to tops?
  - interference effects from NP beyond direct reach of LHC?

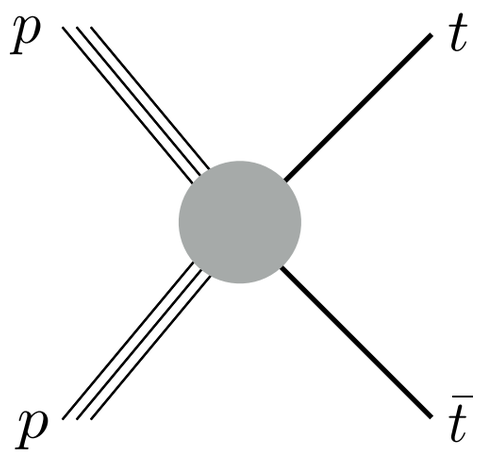

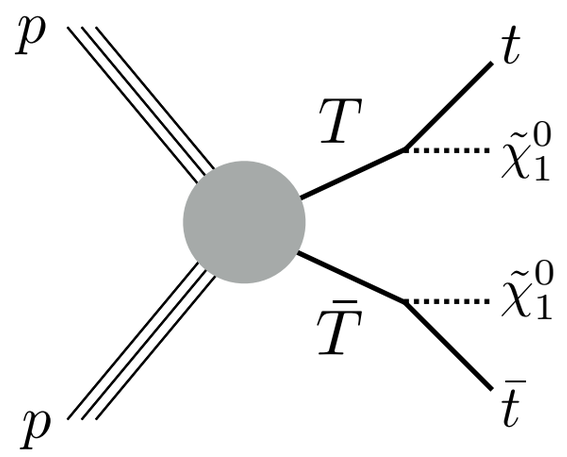

- **LHC @13 TeV opens new window on spin properties**
  - hugely increased statistical precision
  - opportunity for increasingly differential measurements

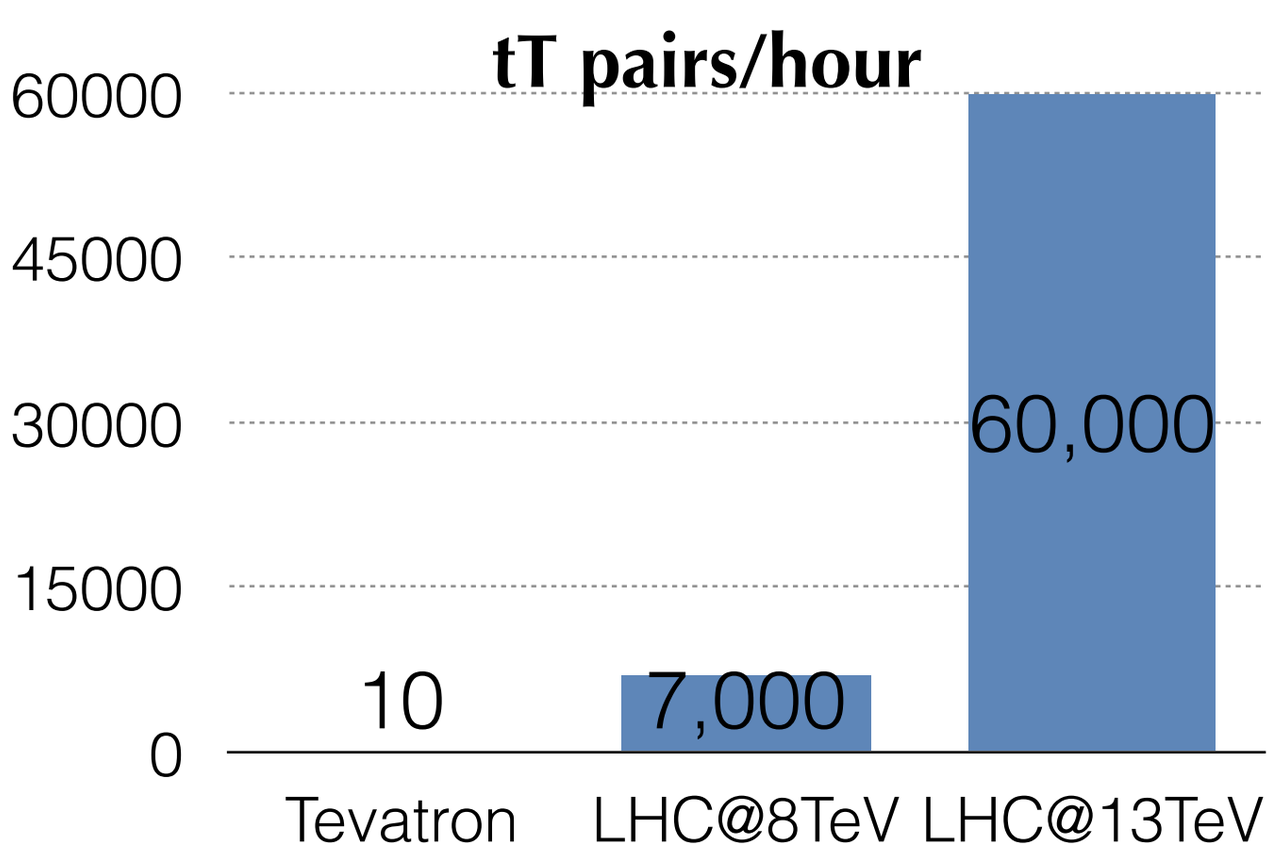

$t\bar{t}$ spin correlations in the SM

+1 **spin correlation strength** **-1**

Dominant mode near threshold (dominant at high top p_T)

in $t\bar{t}$ CM frame

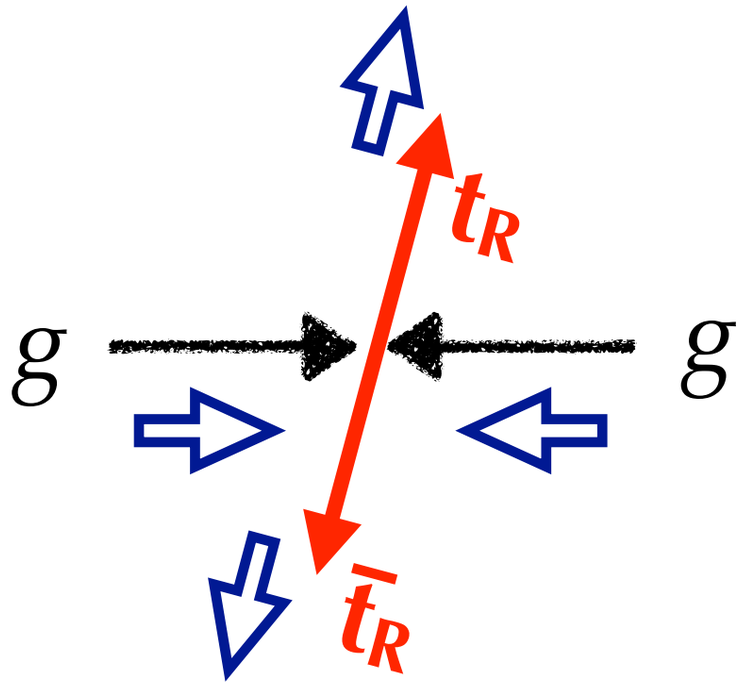

Same helicity tops

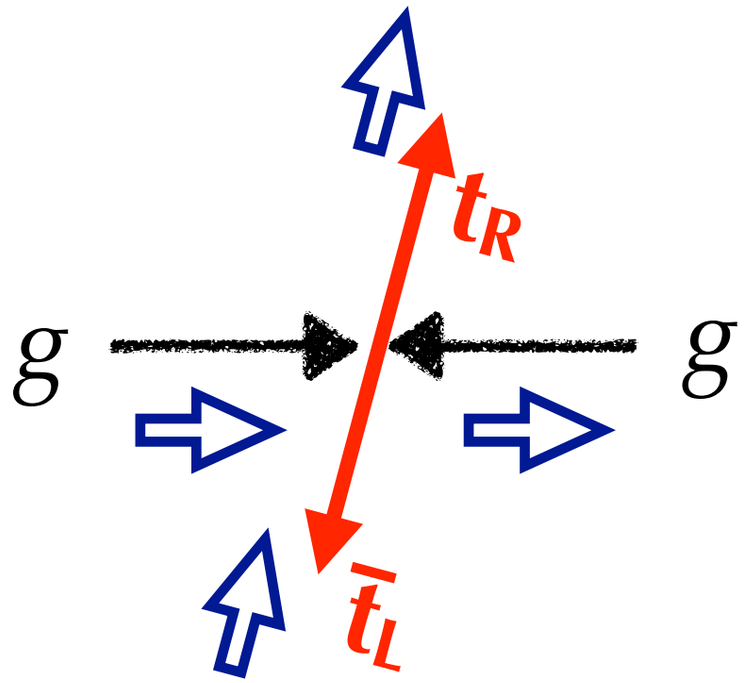

Opposite helicity tops

- But negligible top polarisation because QCD is P-conserving

tT spin density matrix

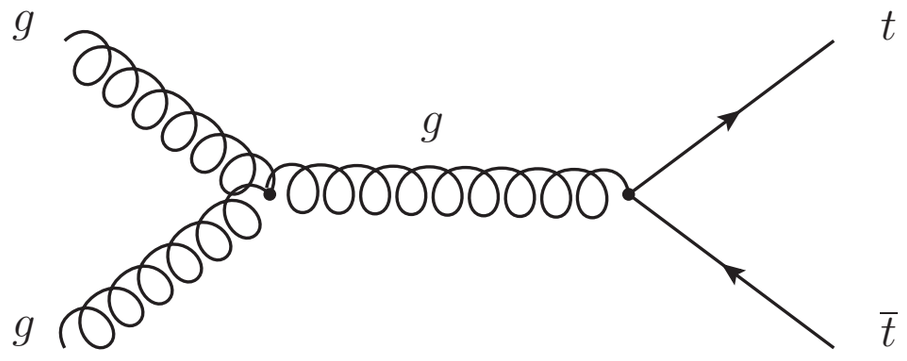

Bernreuther, Heisler & Si, 1508.05271

- Spin properties encoded in tT production spin density matrix ρ:

$$\rho \propto \left[\tilde{A}\,\mathbb{I}\otimes\mathbb{I} + \tilde{B}_i^+\,\sigma^i\otimes\mathbb{I} + \tilde{B}_i^-\,\mathbb{I}\otimes\sigma^i + \tilde{C}_{ij}\,\sigma^i\otimes\sigma^j\right]$$

$$\tilde{B}_i^+ = \langle 2S^i\rangle,\ \tilde{B}_i^- = \langle 2\bar{S}^i\rangle,\ \tilde{C}_{ij} = \langle 4S^i\bar{S}^j\rangle$$

- **6 $B_i^{\pm}$** and **9 C_{ij} functions** of partonic initial state and production kinematics
  - all **sensitive to NP in production,** each can be **classified by discrete symmetries** (including P and CP)
  - Objective is to measure them all! All we have to do is measure the top and antitop spin in each event …

Polarised top quark decay

- The top quark's spin determines the angular distribution of its daughters when it decays

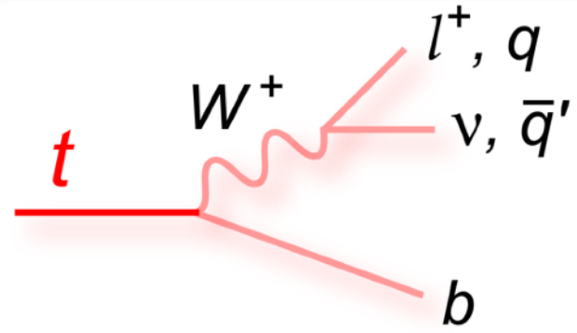

top rest frame

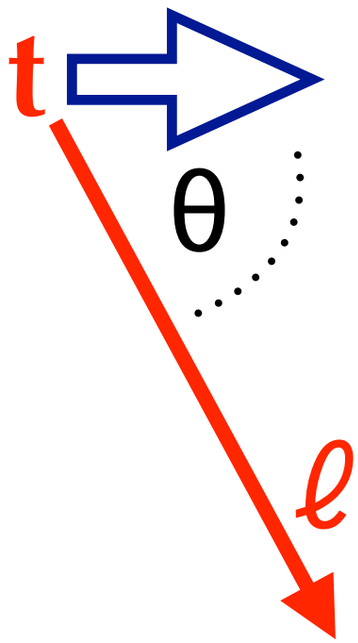

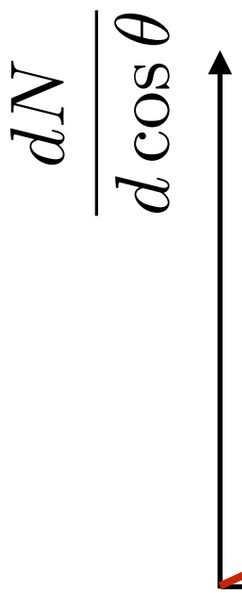

$$\frac{1}{2}(1 + \kappa \cos\theta)$$

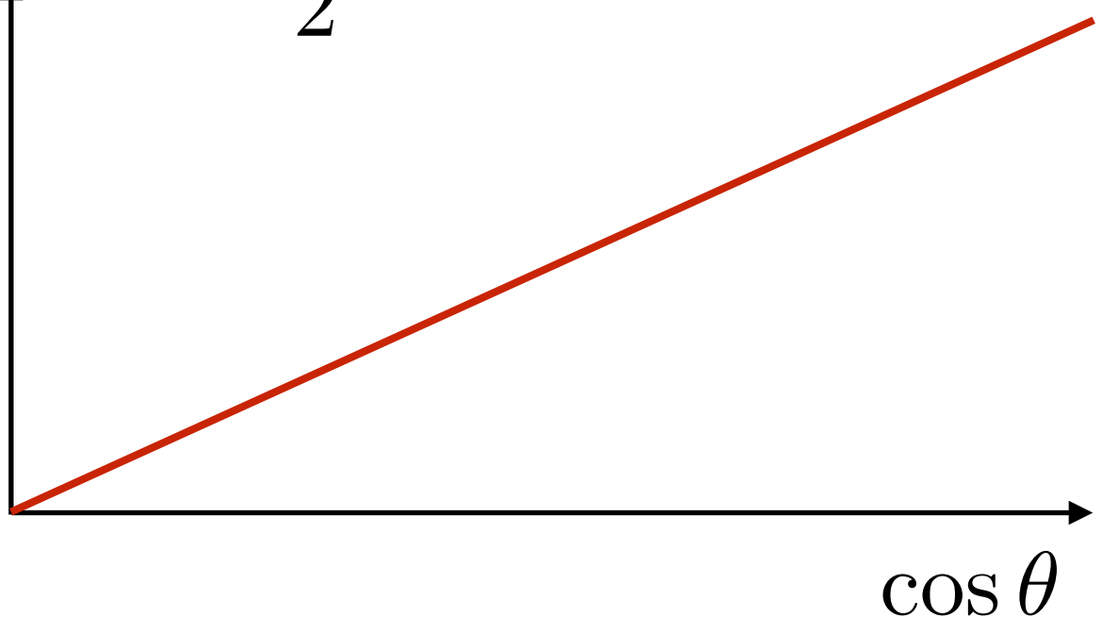

- ℓ has best spin analysing power, κ=1
  - **ℓ preferentially produced in top spin direction**
  - **lepton 3-momentum is a good proxy for the top spin!**

$t\bar{t}$ dilepton channel

- **Dilepton channel** best choice because **lepton is best spin analyser**
  - **2 leptons + 2 jets +** E_T^{miss} **from undetected neutrinos**

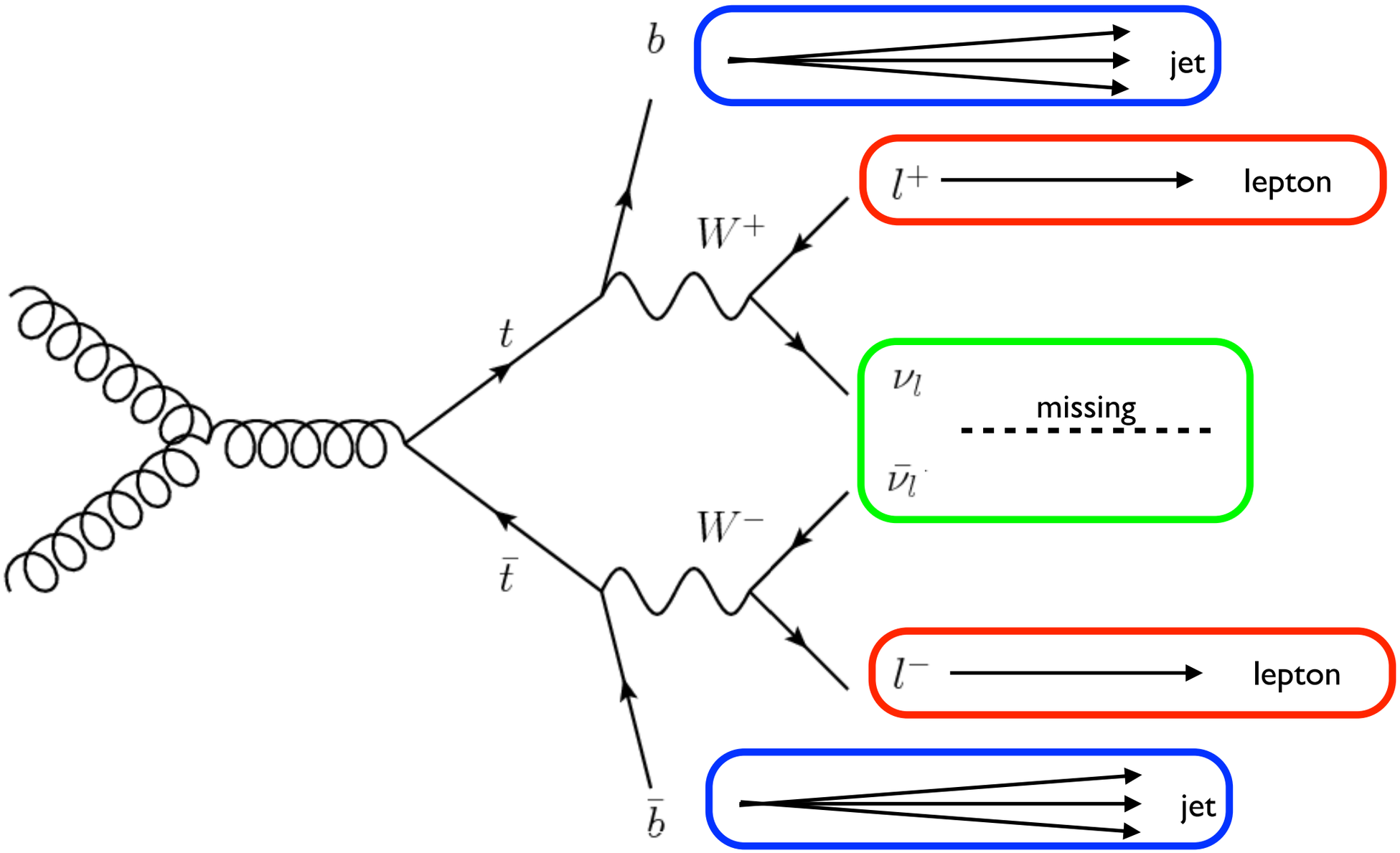

- **>90% pure sample of dileptonic** $t\bar{t}$ **events after selection**

Dilepton angular distribution

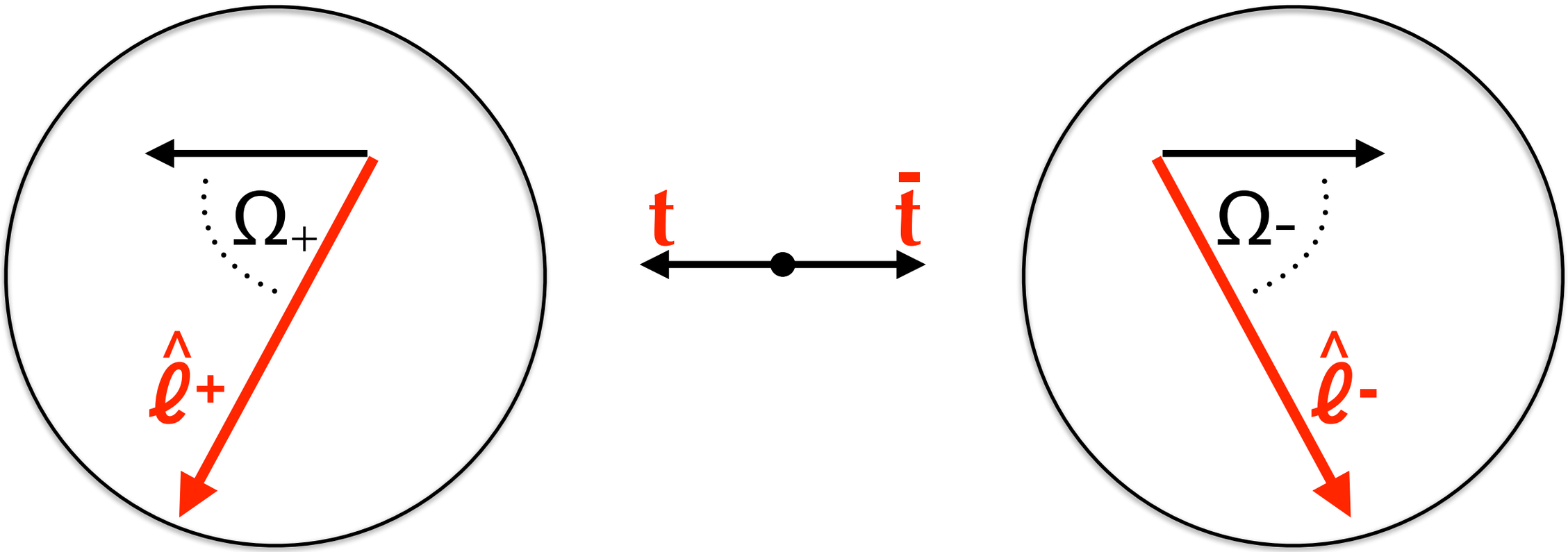

$$\frac{1}{\sigma}\frac{d\sigma}{d\Omega_+ d\Omega_-} = \frac{1}{(4\pi)^2}\left(1 + \mathbf{B}^+ \cdot \hat{\ell}^+ + \mathbf{B}^- \cdot \hat{\ell}^- - \hat{\ell}^+ \cdot \mathbb{C} \cdot \hat{\ell}^-\right)$$

- Change variables to single-differential cross-section for each coefficient, and measure 1D distributions:
  - 6 for the polarisation coefficients from the 3-vectors $\mathbf{B}^{+/-}$
  - 9 for the spin correlation coefficients from the 3x3 matrix $\mathbf{C}$

Dilepton angular distribution

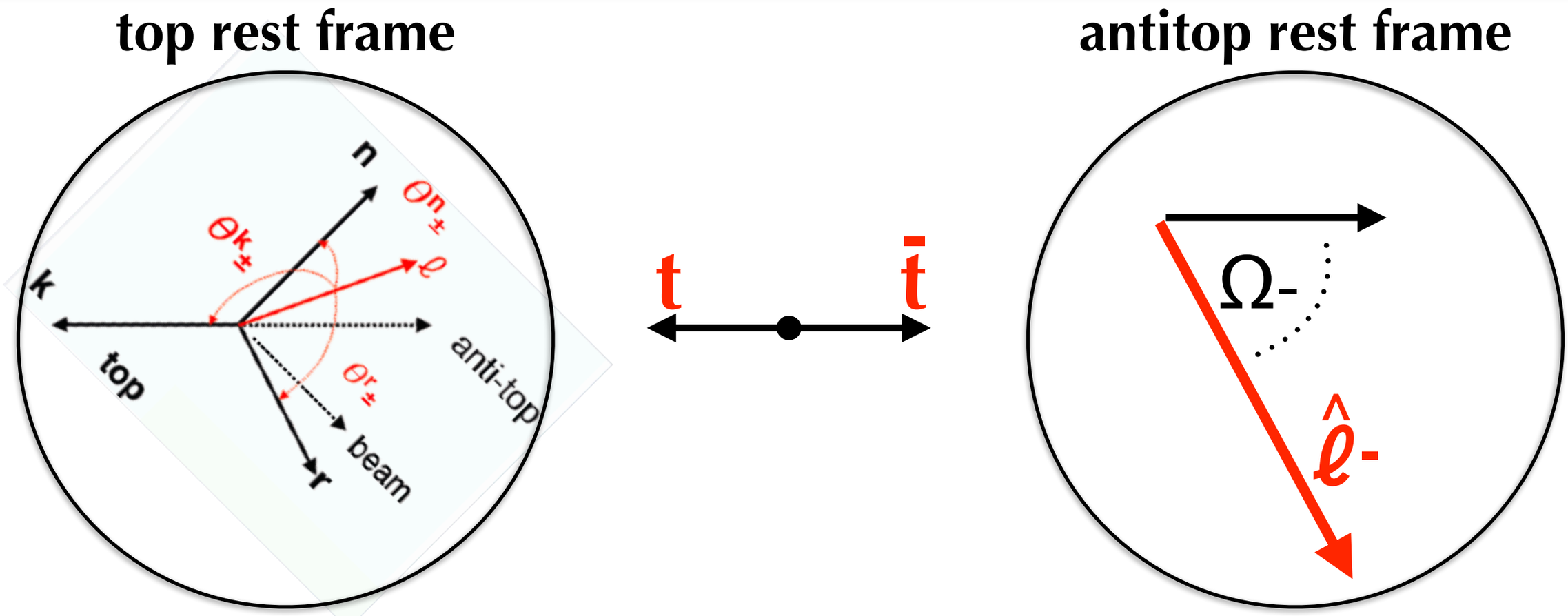

$$\frac{1}{\sigma}\frac{d\sigma}{d\Omega_+ d\Omega_-} = \frac{1}{(4\pi)^2}\left(1 + \mathbf{B}^+ \cdot \hat{\ell}^+ + \mathbf{B}^- \cdot \hat{\ell}^- - \hat{\ell}^+ \cdot \mathbb{C} \cdot \hat{\ell}^-\right)$$

- 1D angular distributions have simple form

$$\frac{1}{\sigma}\frac{d\sigma}{dx} = \frac{1}{2}\left(1 + [\mathbf{Coef.}]\, x\right) f(x)$$

Angular distributions (polarisation)

- Coefficients of the **$B^{\pm}$** vectors measured from the below distributions (shown for the SM)

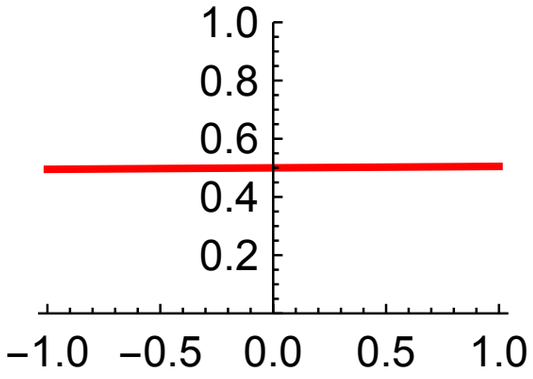

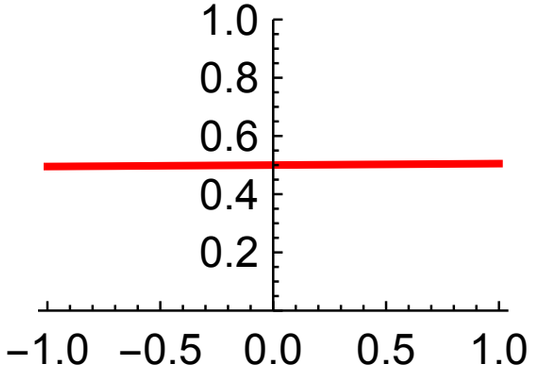

$\Rightarrow B_i^+$

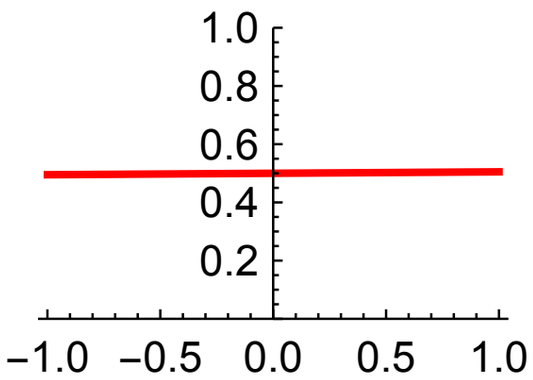

$\cos\theta_i^+$

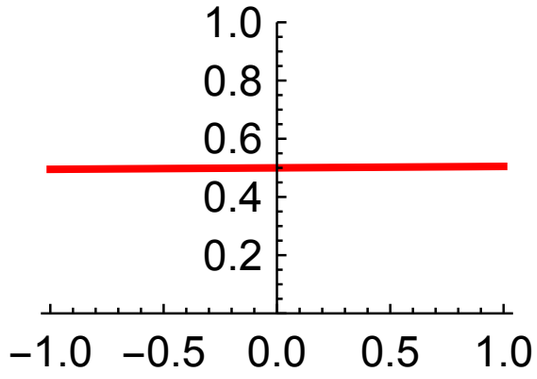

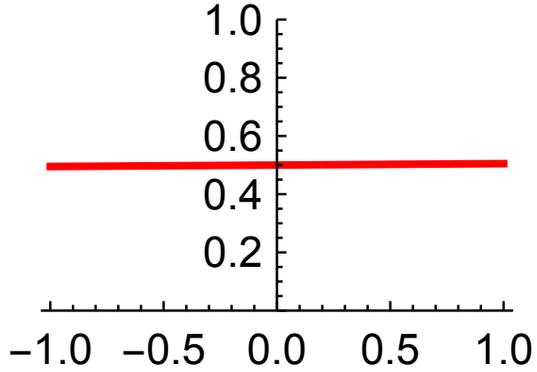

$\Rightarrow B_i^-$

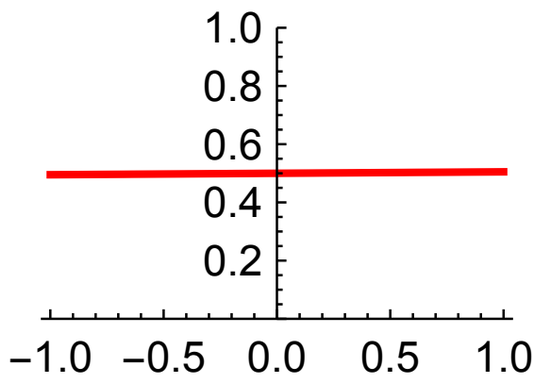

$\cos\theta_i^-$

Angular distributions (spin correlation)

- Coefficients of the **C** matrices measured from the below distributions (shown for the SM)

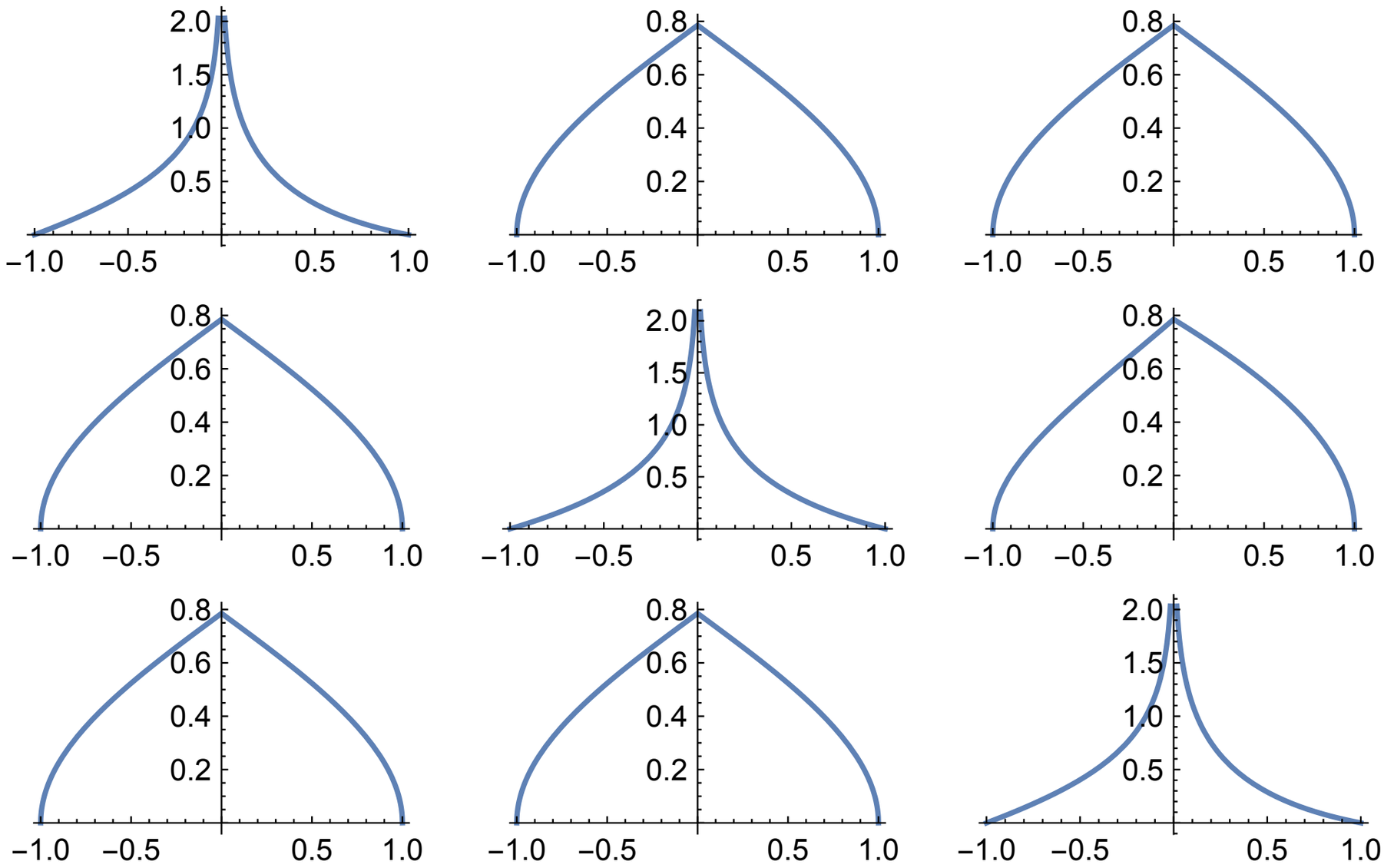

$\Rightarrow C_{ij}$

$$x = \cos\theta_i^+ \cos\theta_i^- \;\; [\text{diag}]; \;\; x = \cos\theta_i^+ \cos\theta_j^- \pm \cos\theta_j^+ \cos\theta_i^- \;\; [\text{nondiag}]$$

Interpretation

- Coefficients probe **most of the lowest-order EFT operators** relevant to tT production
  - each coefficient is sensitive to 1, 2, or 3 of these operators
  - can be disentangled in a combined fit

Bernreuther et al.
1508.05271

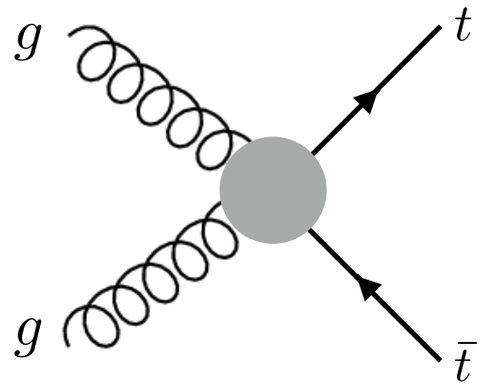

LHCtopWG EFT
document 1802.07237

- tT spin measurements sensitive to some interesting models that could still be in LHC direct production reach
  - ‘stealthy’ SUSY
  - heavy Higgs resonances
  - top-philic DM
  - **looking for more ideas!**

Bernreuther et al.
1702.06063

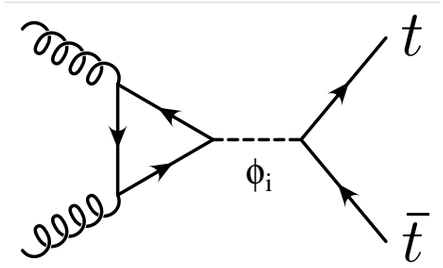

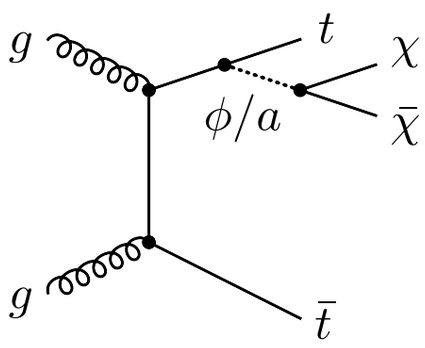

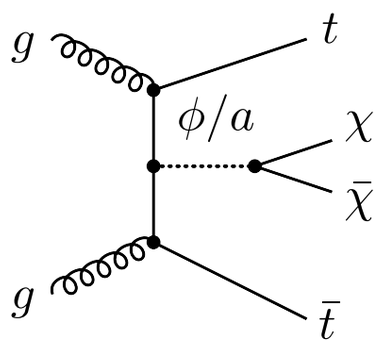

Haisch et al.
1611.09841

General analysis strategy

- Dilepton event selection
- tT system reconstruction
  - 6 unknowns (neutrino momenta) constrained by measured MET and assumed m_t and m_W
- measure differential cross section distributions in bins
- background estimation
  - **tW** single-top production dominant background
- **compare data to BSM predictions** and set limits
  - use reconstruction-level data?
  - correct for detector effects and acceptance?
    - unfolding

Reconstruction-level data

- Want to compare the data to BSM predictions

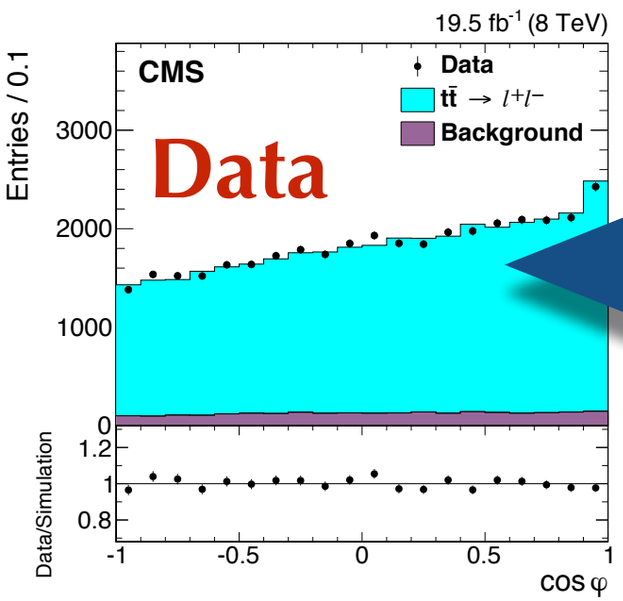

Geometric acceptance

Parton level

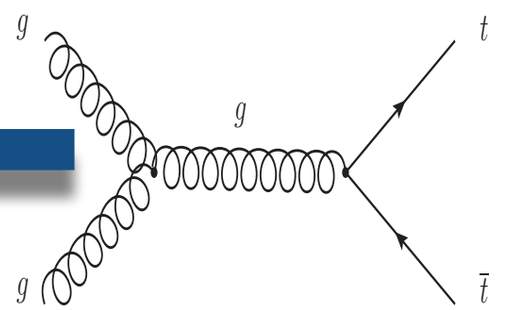

- Huge parameter space of models: impractical to perform full simulation chain
  - and also makes our results inaccessible for future models (or more sophisticated predictions)
- Also difficult to include in a global analysis of all EFT operators

Unfolding to parton level

- To measure the coefficients directly, must **correct to parton-level**

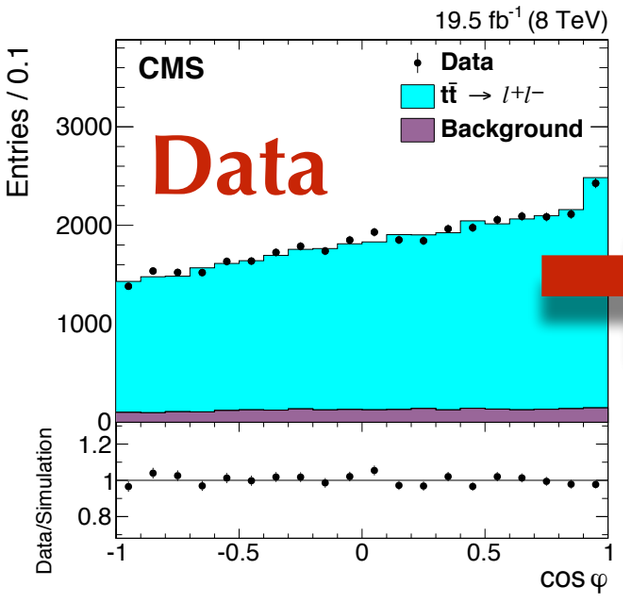

Geometric acceptance

Parton level

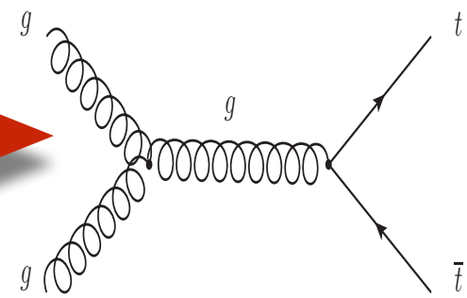

ADVANTAGES	DISADVANTAGES
Compare with fixed-order calculations	Model-dependence of parton shower
Combine with other experiments	Model-dependence of extrapolation
Can be used as part of global fit	Difficult to accurately estimate systematics

Unfolding to particle level

- To reduce the model-dependence, we can unfold to **particle-level** and **minimise the acceptance extrapolation**

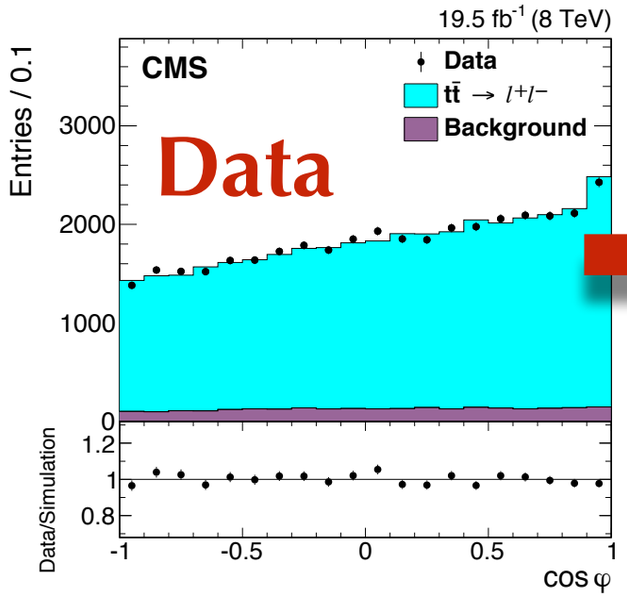

Particle level

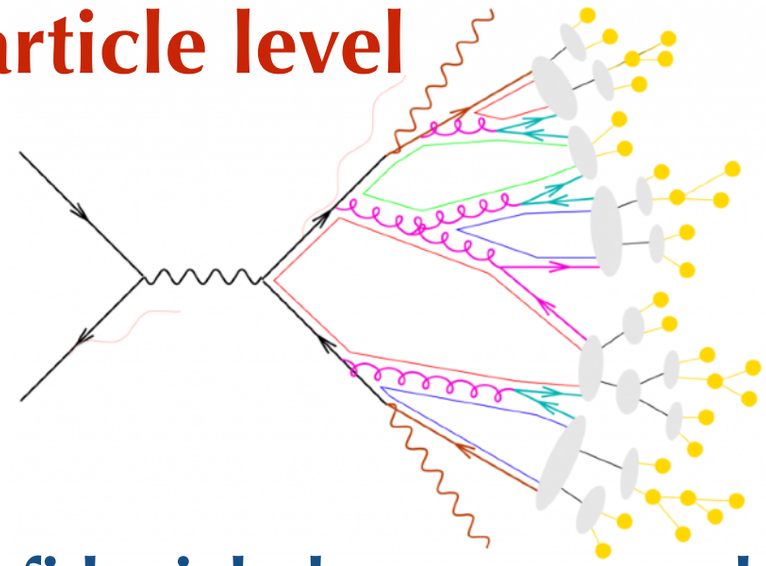

(in fiducial phase space only)

ADVANTAGES	DISADVANTAGES
Detector simulation (slow) not needed for BSM samples	Still have to produce particle-level MC
Results less dependent on model used for unfolding	No fixed-order calculations
Combinations, global fit	

Results

(8 TeV data, parton-level)

Polarisation

- **Lepton direction** in parent top CM a good **proxy for the top spin**
  - spin measured along 'k' axis, defined by top momentum (helicity basis)
- Two measurements per event (from ℓ^+ and ℓ^-), combined assuming CP conservation
  - **$B_k = (-2.2 \pm 1.5 \pm 5.6)\%$**
  - JES dominant systematic
- Measurements along other two axes (r and n) not performed by CMS at 8 TeV

Phys. Rev. D 93 (2016) 052007

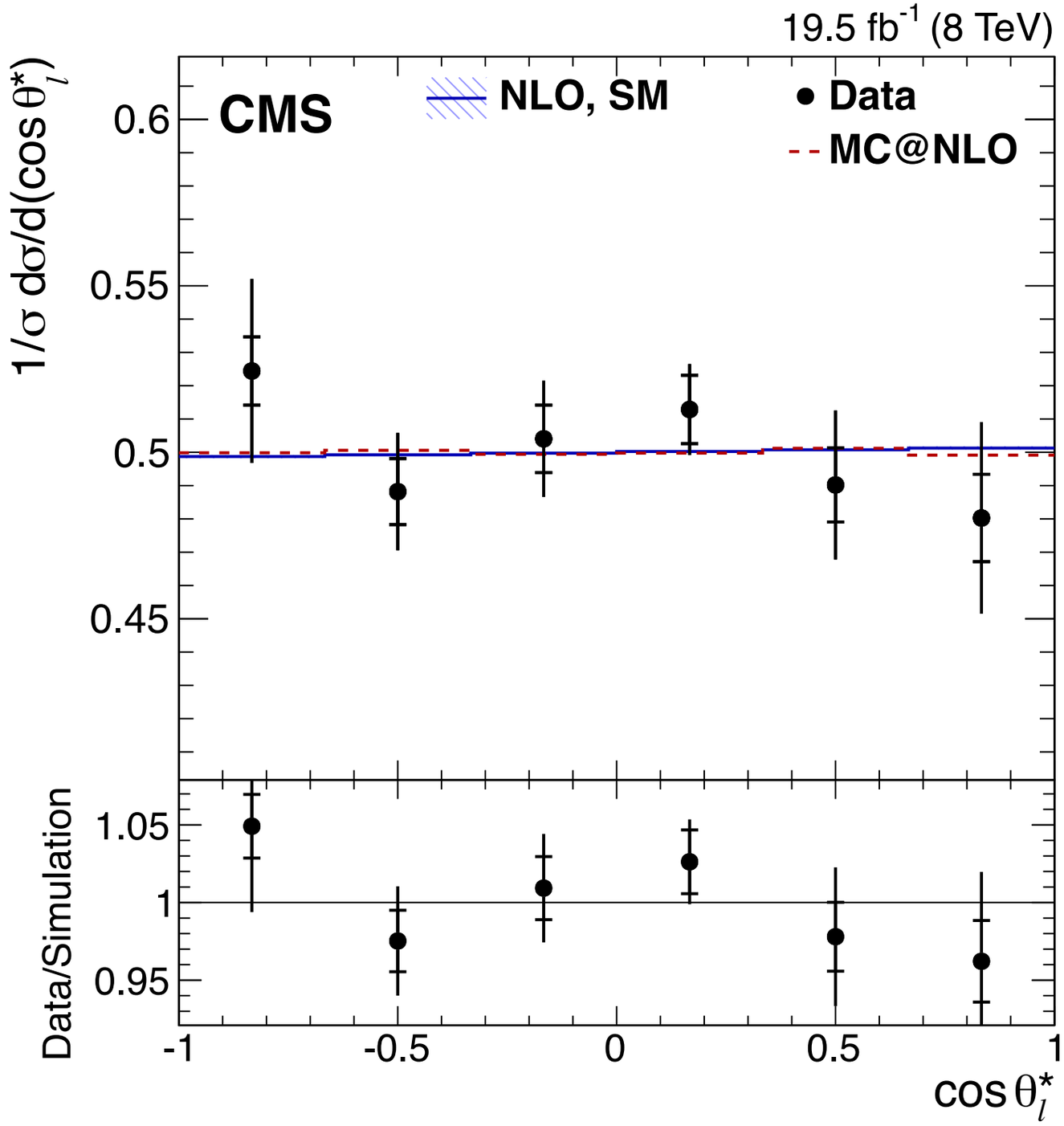

Spin correlations

- **left**: distribution corresponding to **product of top spins (k axis)**, $\cos\theta^*_{\ell+}\cos\theta^*_{\ell-}$
- **right**: cosine of **opening angle between the spins**, $\varphi = \angle(\hat{\ell+}, \hat{\ell-})$

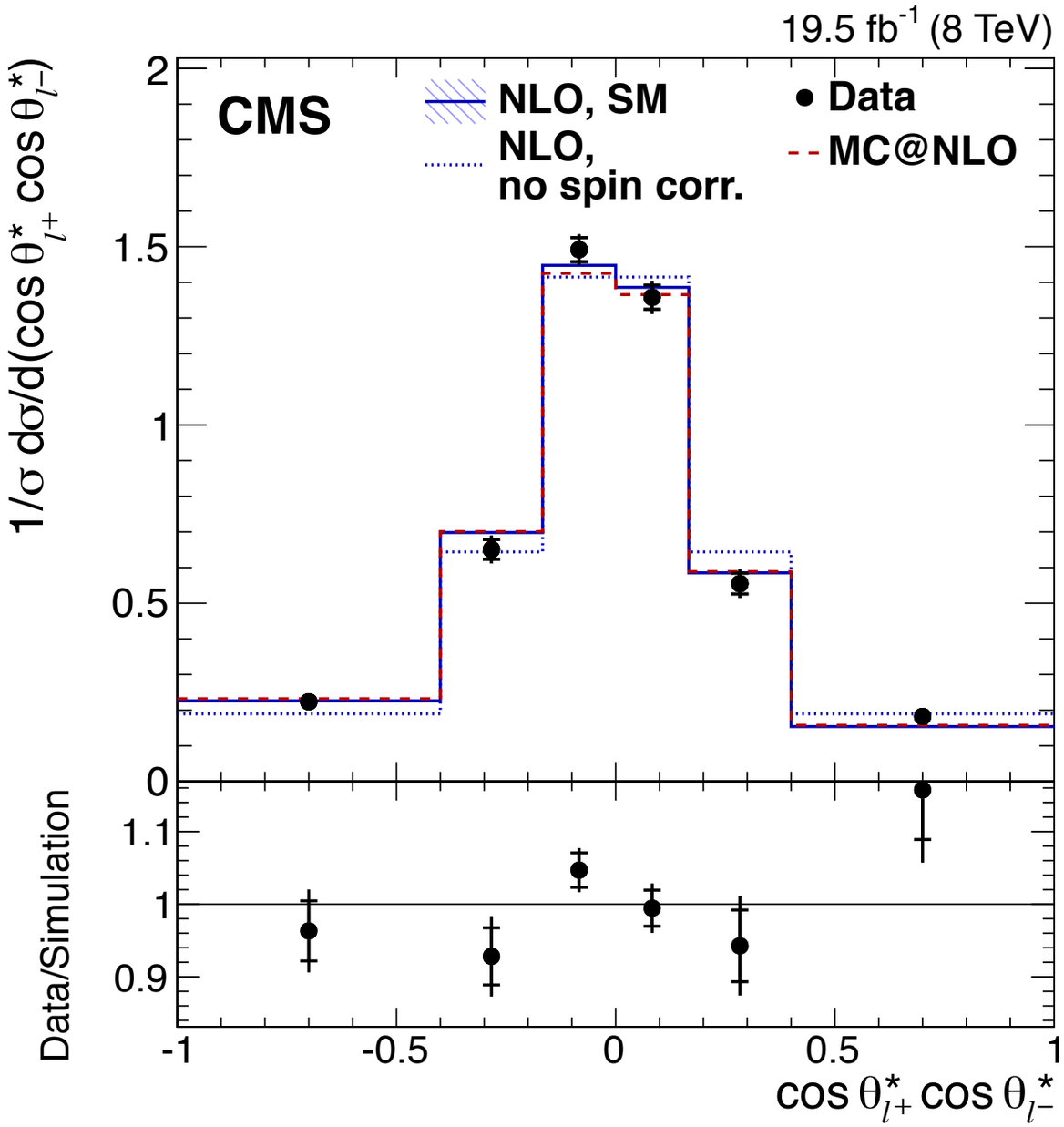

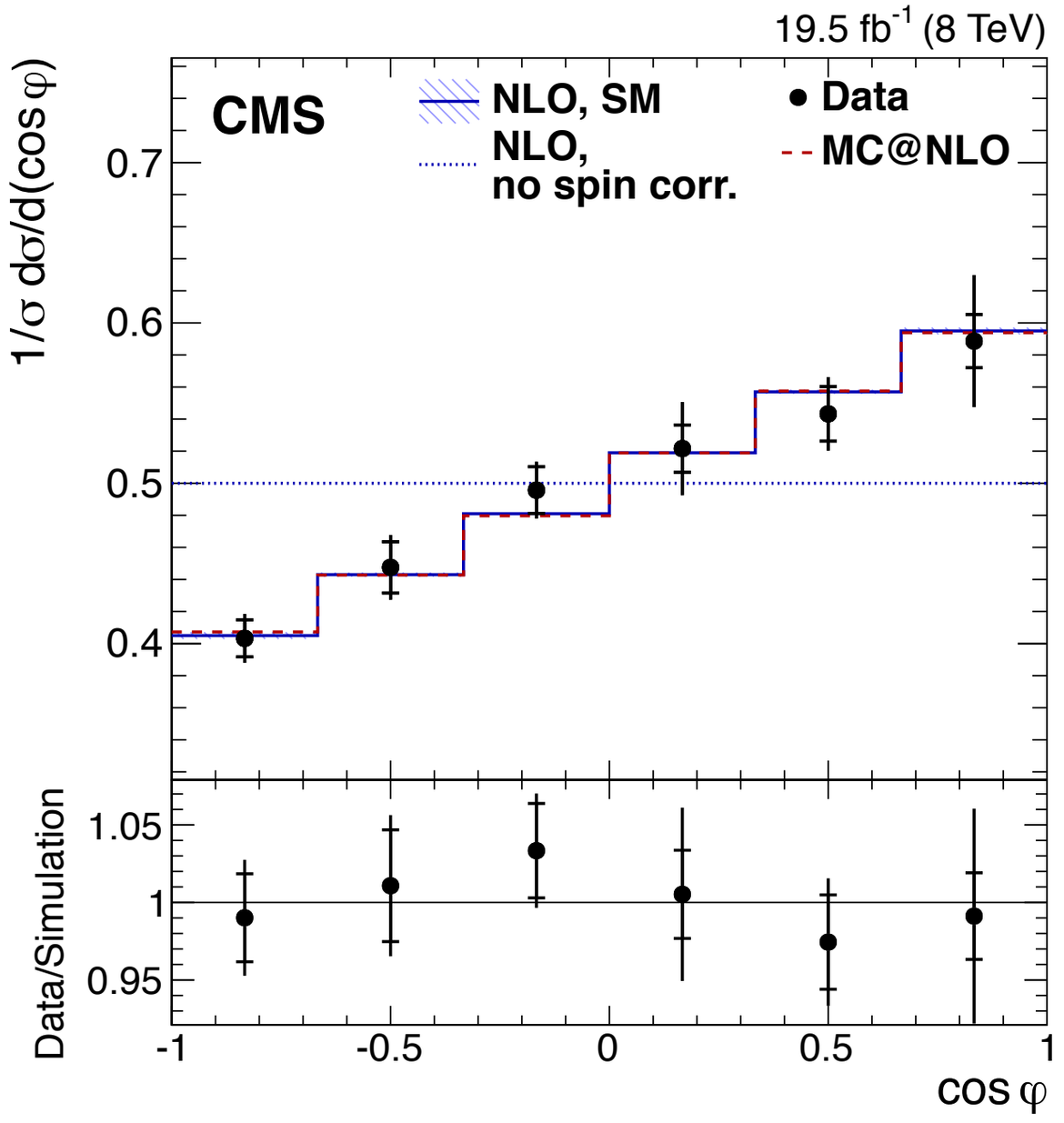

- $C_{kk} = 0.28 \pm 0.05 \pm 0.06$
- $D = (C_{kk}+C_{rr}+C_{nn})/3 = 0.20 \pm 0.02 \pm 0.02$

CMDM results

- Limited EFT interpretation done using the 8 TeV data
  - will be much more extensive at 13 TeV

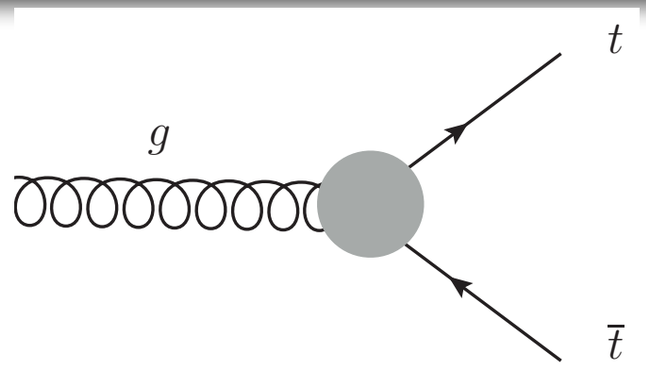

- **95% CL Limits on CMDM operators** from comparing measurements to theoretical predictions:
  - **-0.053< Re(CMDM) <0.026**

⇐

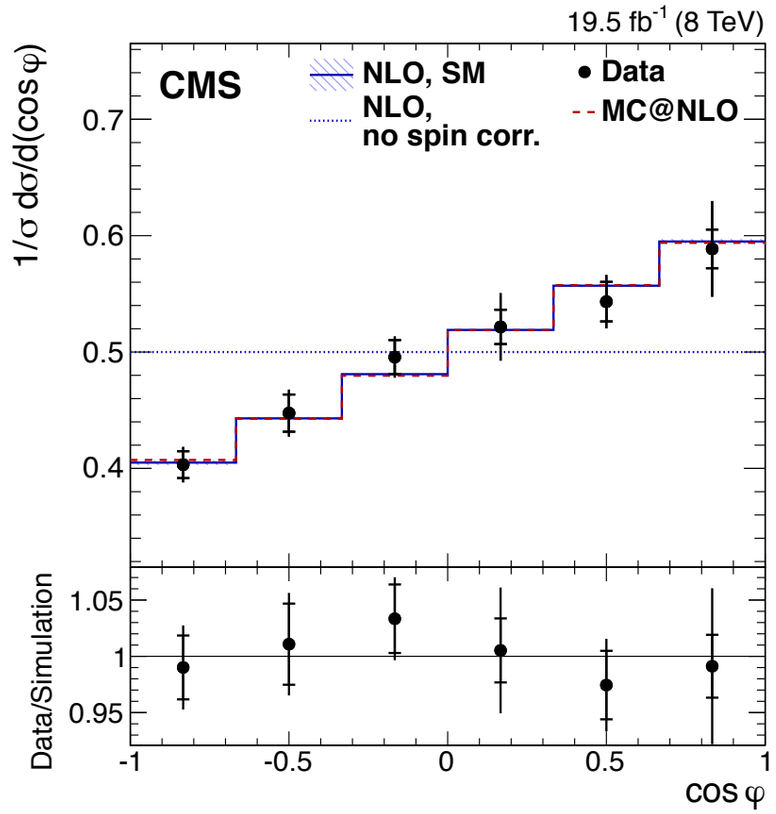

- Expect significantly improved sensitivity in 13 TeV data
  - more optimised analysis
  - combination of results from all sensitive distributions
  - double-differential distributions no longer stat limited

[Phys. Rev. D 93 (2016) 052007]

Summary

- Precision top quark spin measurements are a powerful probe of new physics
  - and complementary to other approaches
- Exciting advances expected in 13 TeV results
  - results at particle-level for use in global analysis
  - fully exploit double-differential distributions
  - measure all coefficients of the spin density matrix for the first time at CMS!

Backup

LHC collider

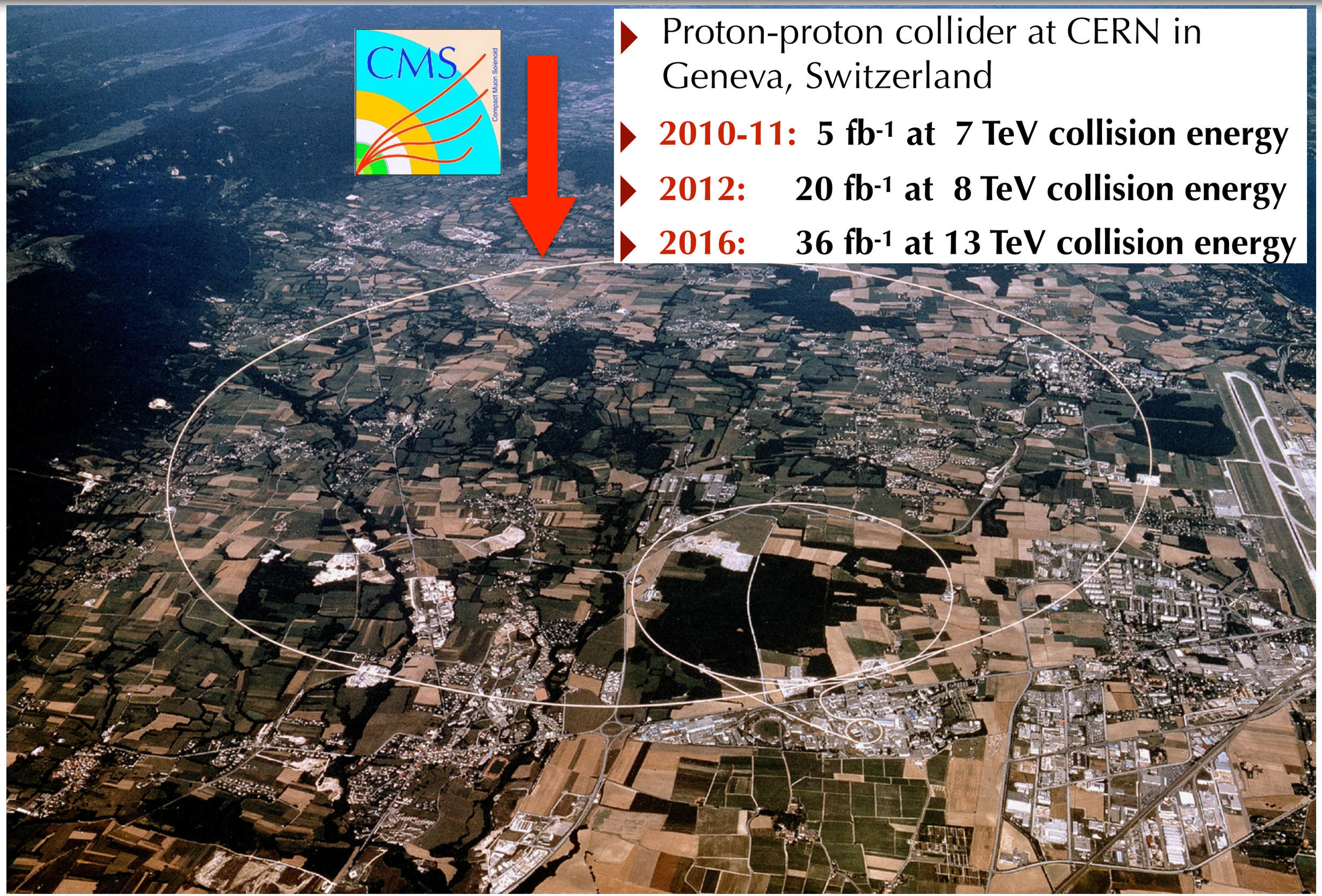

- Proton-proton collider at CERN in Geneva, Switzerland
- **2010-11: 5 fb^{-1} at 7 TeV collision energy**
- **2012: 20 fb^{-1} at 8 TeV collision energy**
- **2016: 36 fb^{-1} at 13 TeV collision energy**

CMS detector

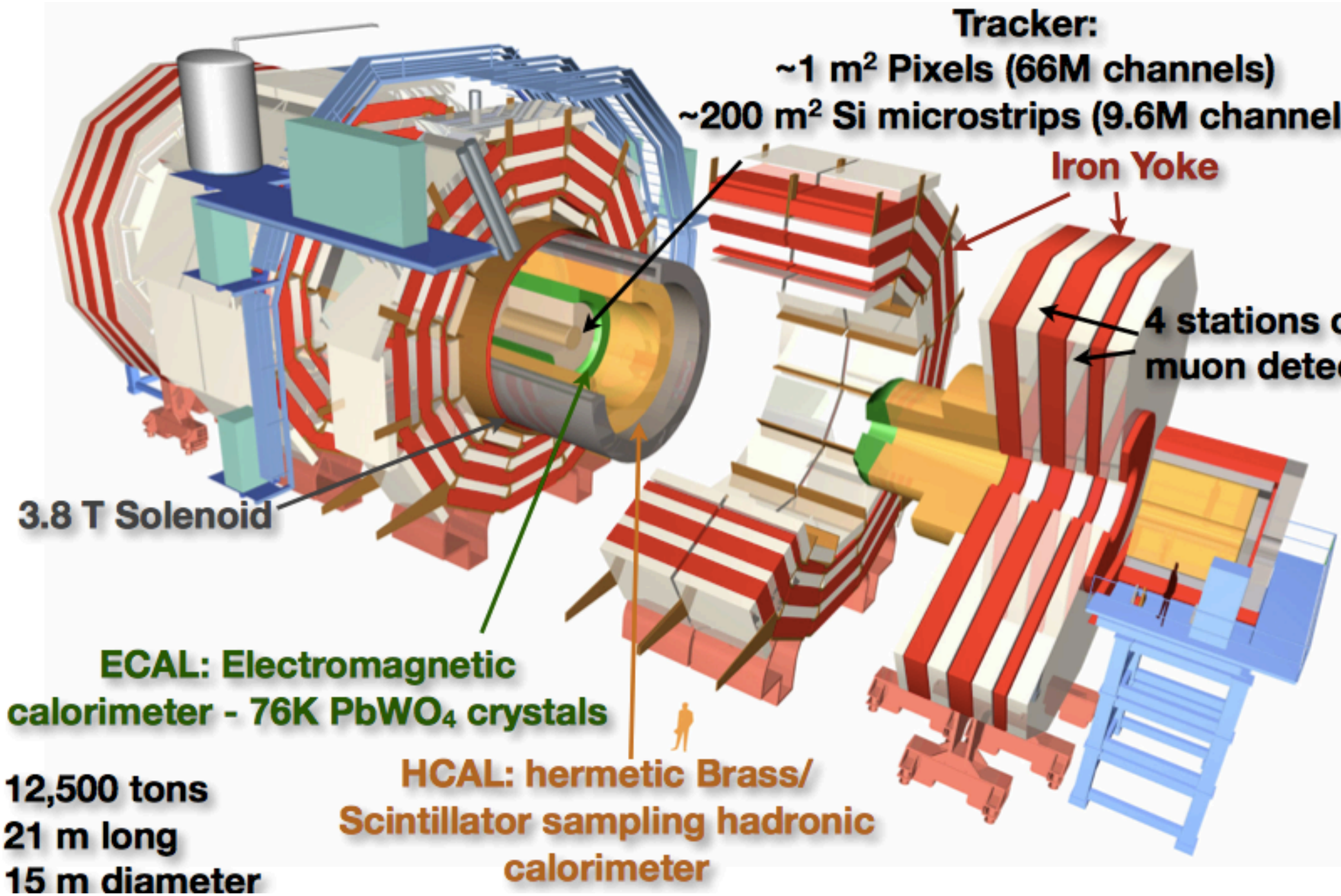

- Highly complex multi-purpose detector to probe diverse range of final states
- Hermetic → attribute **momentum imbalance "** $\mathbf{E_T^{miss}}$ **"** to **undetected particles**

$t\bar{t}$ decay channels

- Decay channels categorised based on how the two W bosons decay

dilepton (l=e,μ)
6%
small branching fraction but small backgrounds

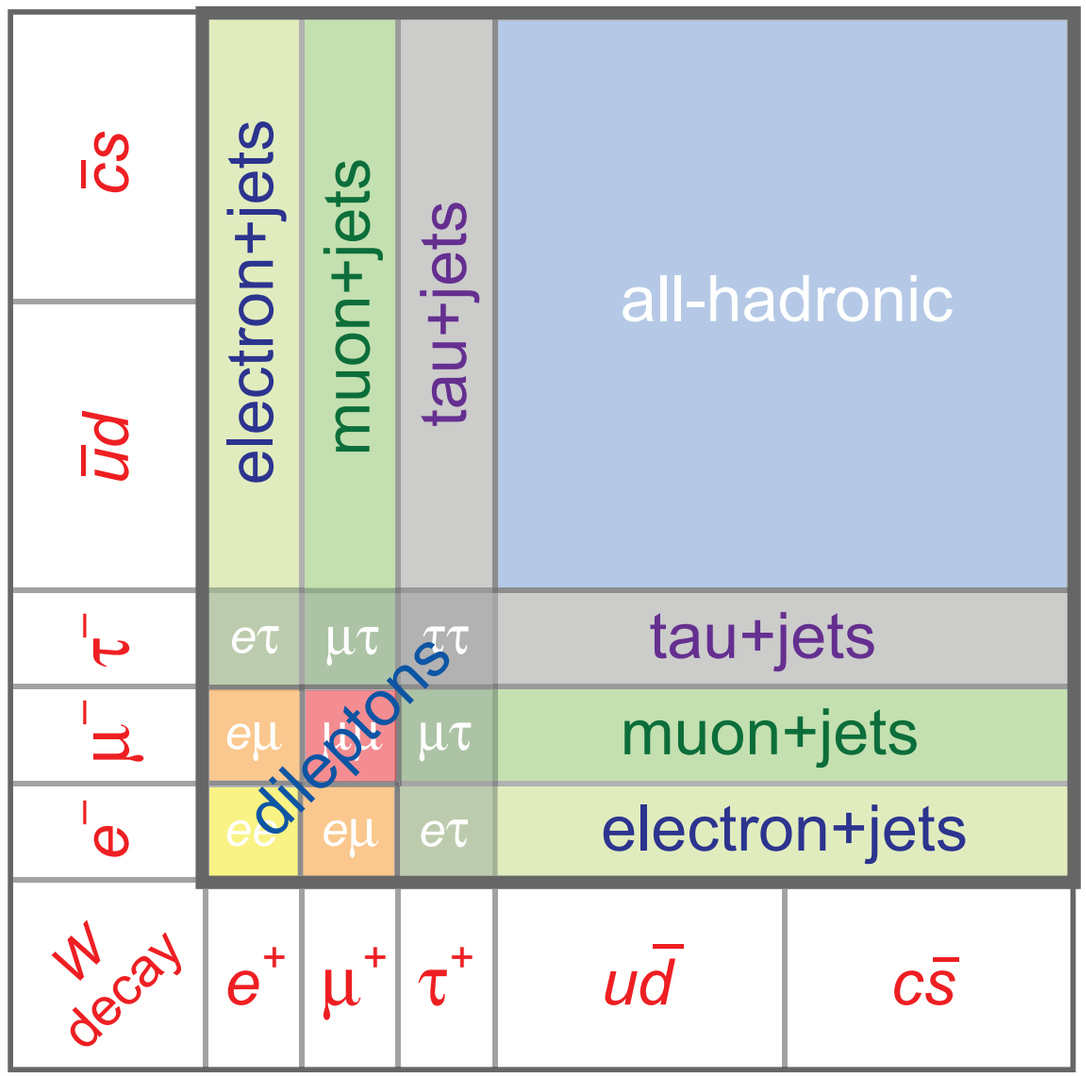

all-hadronic
46%
largest branching fraction but largest backgrounds

lepton+jets (l=e,μ)
34%
Large branching fraction and manageable backgrounds

- Talk focuses on the **dilepton channel**
  - **extremely clean, very high purity** (only **~7% background** contamination)
    - makes measurements very **insensitive to uncertainties in the background**

Dilepton $t\bar{t}$ selection

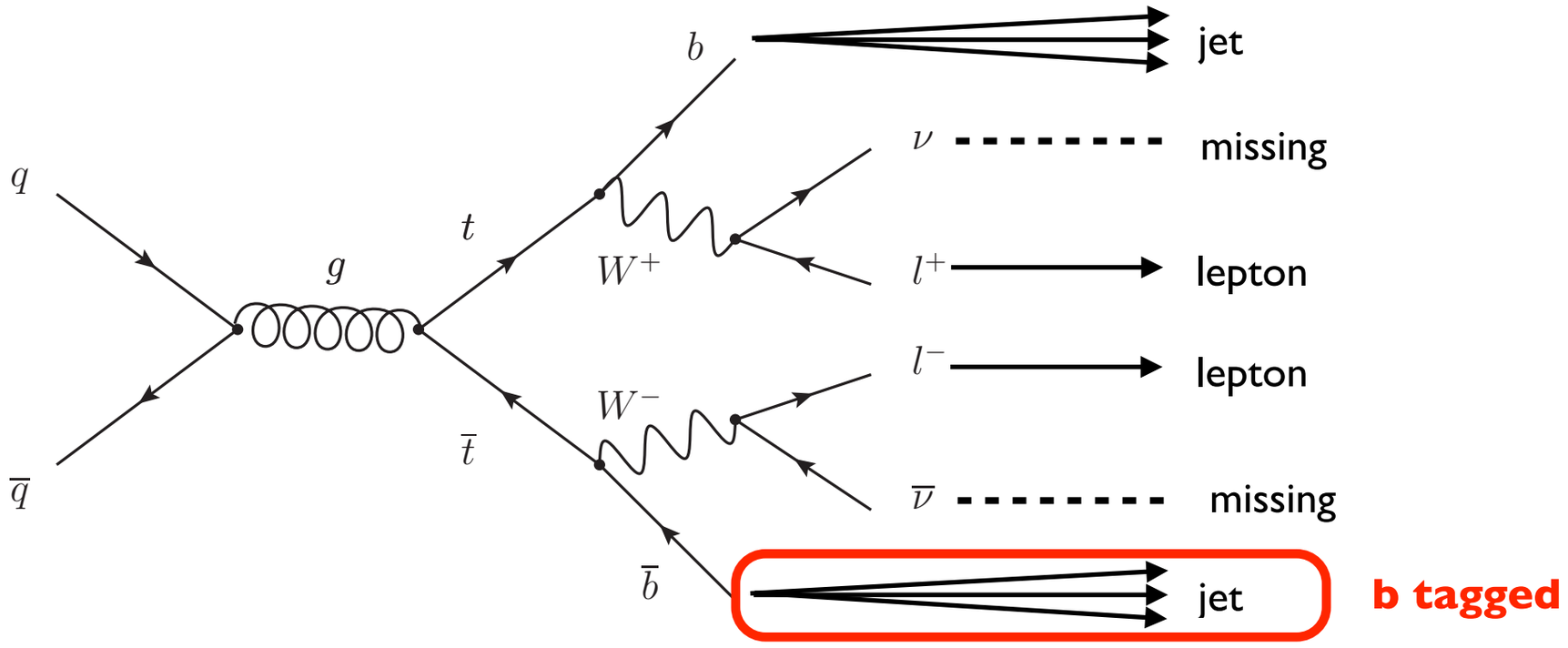

- Selection is designed to **reject events other than $t\bar{t}$ → dileptons**
  - **2 opposite-charged isolated leptons, ≥2 jets with ≥1 b tag**
  - **missing transverse energy (MET) > 40 GeV** (ee and μμ channels only)
- Selected event sample is **93% pure**
  - measurements very insensitive to uncertainties in the background

Solving the top pair kinematics

- Direct spin measurement requires **reconstruction of $t\bar{t}$ system**

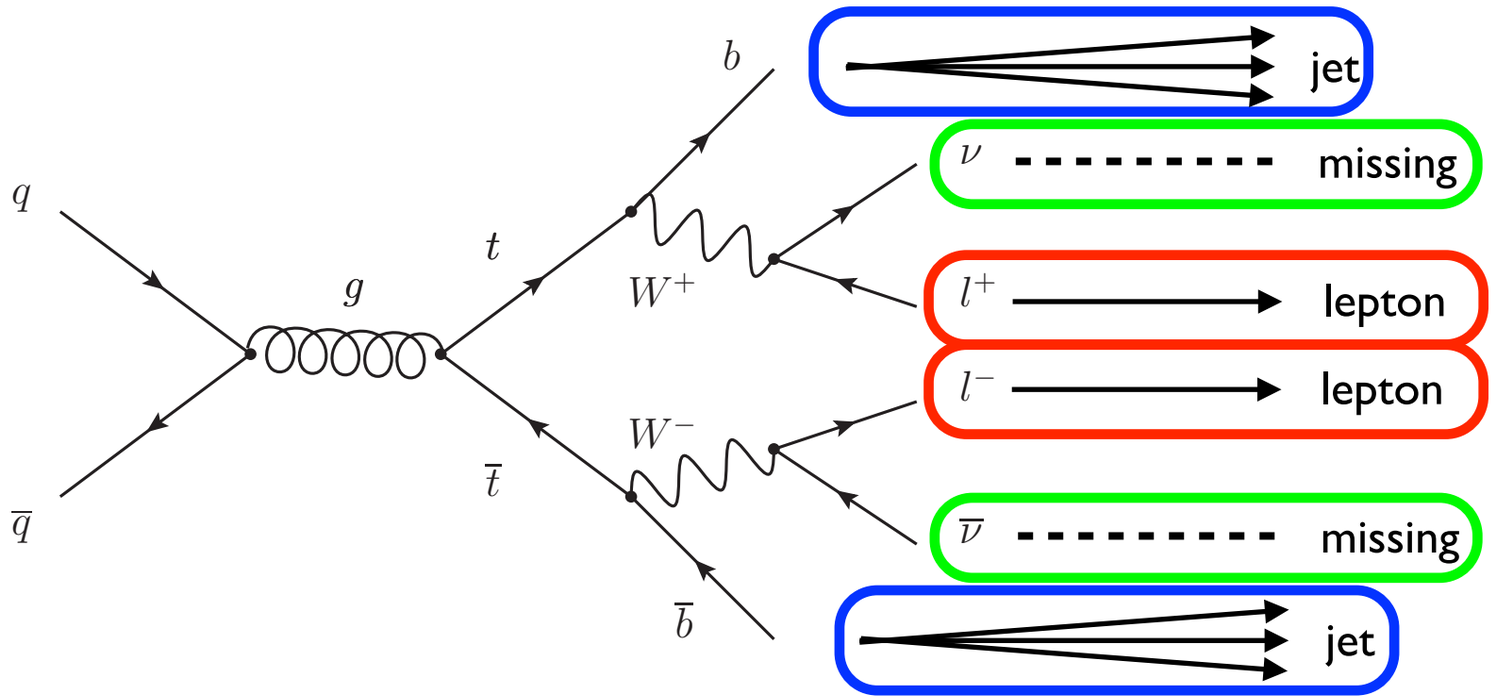

- Neutrino momenta solved analytically using a geometric method
  - Input: **2 highest-pt reconstructed jets**, **2 leptons** and **missing transverse energy**
  - fix top quark mass at 172.5 GeV and W mass at 80.4 GeV
- Up to 8 solutions per event
  - choose most likely based on kinematics
  - take closest approach between MET and sum of neutrino p_T in case of no physical solutions

Unfolding

- Two corrections needed to compare measured distribution to theoretical calculations:
  - **"acceptance"** (from fiducial region of detector with selection cuts to full phase space with no cuts)
  - **"migration"** (to account for differences between true and reconstructed quantities)

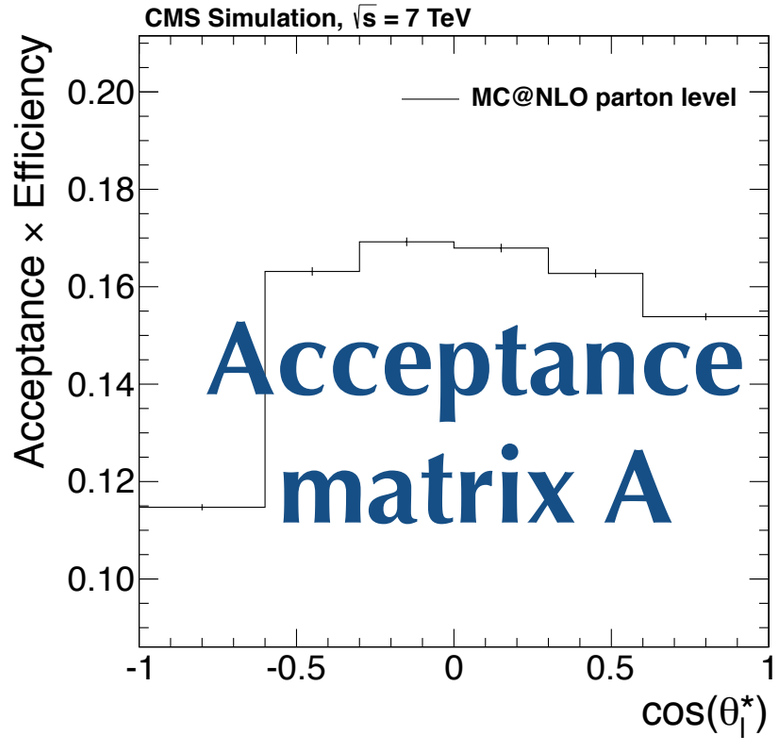

- **Acceptance** and **migration** corrections parameterised by **matrices** that act on measured bins
  - Measured bins **x** related to true bins **y** by **x** = **M A y**
  - equation **inverted** with "regularisation" to suppress statistical fluctuations (TUnfold)

Migration matrix M

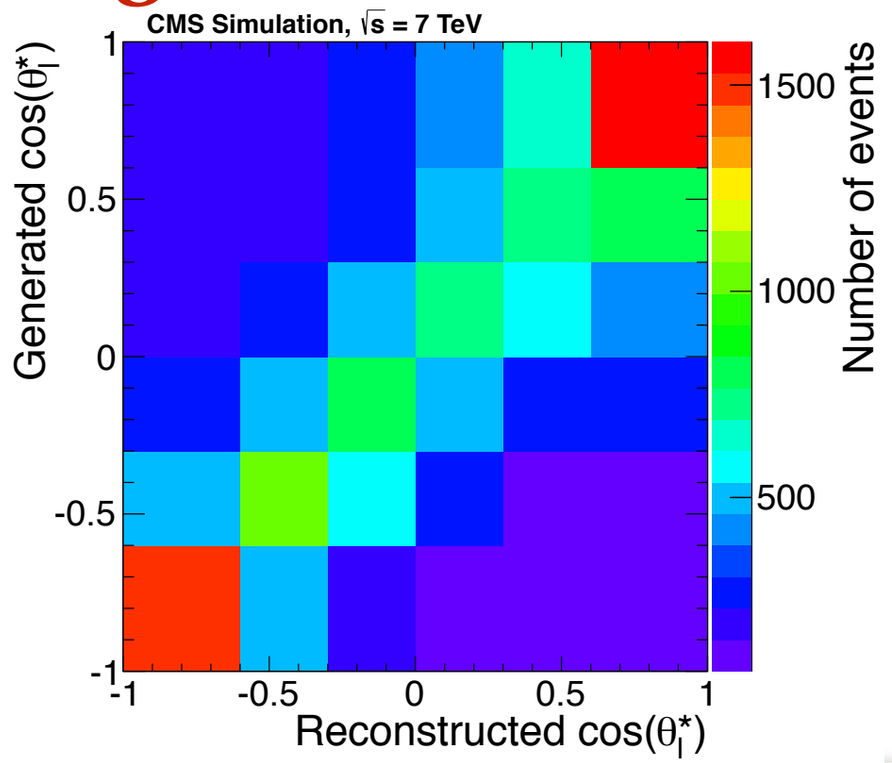

Results tables

Asymmetry variable	Data (unfolded)	MC@NLO simulation	NLO, SM	NLO, no spin corr.
$A_{\Delta\phi}$	$0.094 \pm 0.005 \pm 0.012$	0.113 ± 0.001	$0.107\,^{+0.006}_{-0.009}$	$0.202\,^{+0.006}_{-0.009}$
$A_{\cos\varphi}$	$0.102 \pm 0.010 \pm 0.012$	0.114 ± 0.001	0.114 ± 0.006	0
$A_{c_1c_2}$	$-0.069 \pm 0.013 \pm 0.016$	-0.081 ± 0.001	-0.080 ± 0.004	0
A_P	$-0.011 \pm 0.007 \pm 0.028$	0	0.002 ± 0.001	—
A_P^{CPV}	$0.000 \pm 0.006 \pm 0.005$	0	0	—

Variable	$f_{\mathrm{SM}} \pm (\mathrm{stat}) \pm (\mathrm{syst}) \pm (\mathrm{theor})$	Total uncertainty
$A_{\Delta\phi}$	$1.14 \pm 0.06 \pm 0.13\,^{+0.08}_{-0.11}$	$^{+0.16}_{-0.18}$
$A_{\cos\varphi}$	$0.90 \pm 0.09 \pm 0.10 \pm 0.05$	± 0.15
$A_{c_1c_2}$	$0.87 \pm 0.17 \pm 0.21 \pm 0.04$	± 0.27
$A_{\Delta\phi}$ (vs. $M_{\mathrm{t\bar{t}}}$)	$1.12 \pm 0.06 \pm 0.08\,^{+0.08}_{-0.11}$	$^{+0.12}_{-0.15}$

Systematics

Asymmetry variable	$A_{\Delta\phi}$	$A_{\cos\varphi}$	$A_{c_1c_2}$	A_P	A_P^{CPV}
Experimental systematic uncertainties					
Jet energy scale	0.001	0.005	0.007	0.018	0.001
Jet energy resolution	<0.001	0.001	0.002	0.003	0.002
Lepton energy scale	0.001	0.002	0.005	0.003	<0.001
Background	0.001	0.001	0.001	0.002	<0.001
Pileup	<0.001	<0.001	<0.001	<0.001	<0.001
b tagging efficiency	<0.001	0.001	0.001	0.001	0.001
Lepton selection	0.001	<0.001	<0.001	0.002	<0.001
$\mathrm{t\bar{t}}$ modeling uncertainties					
Parton distribution functions	0.004	0.005	0.005	0.001	<0.001
Top quark p_{T}	0.011	0.006	0.006	0.004	<0.001
Fact. and renorm. scales	0.002	0.003	0.005	0.002	0.002
Top quark mass	0.001	0.001	0.007	0.008	0.001
Hadronization	0.001	0.004	0.005	0.019	0.003
Unfolding (simulation statistical)	0.002	0.005	0.006	0.003	0.003
Unfolding (regularization)	<0.001	<0.001	<0.001	<0.001	<0.001
Total systematic uncertainty	0.012	0.012	0.016	0.028	0.005

Differential measurements

- Spin variables measured **differentially** wrt $M_{t\bar{t}}, |y_{t\bar{t}}|, p_T^{t\bar{t}}$

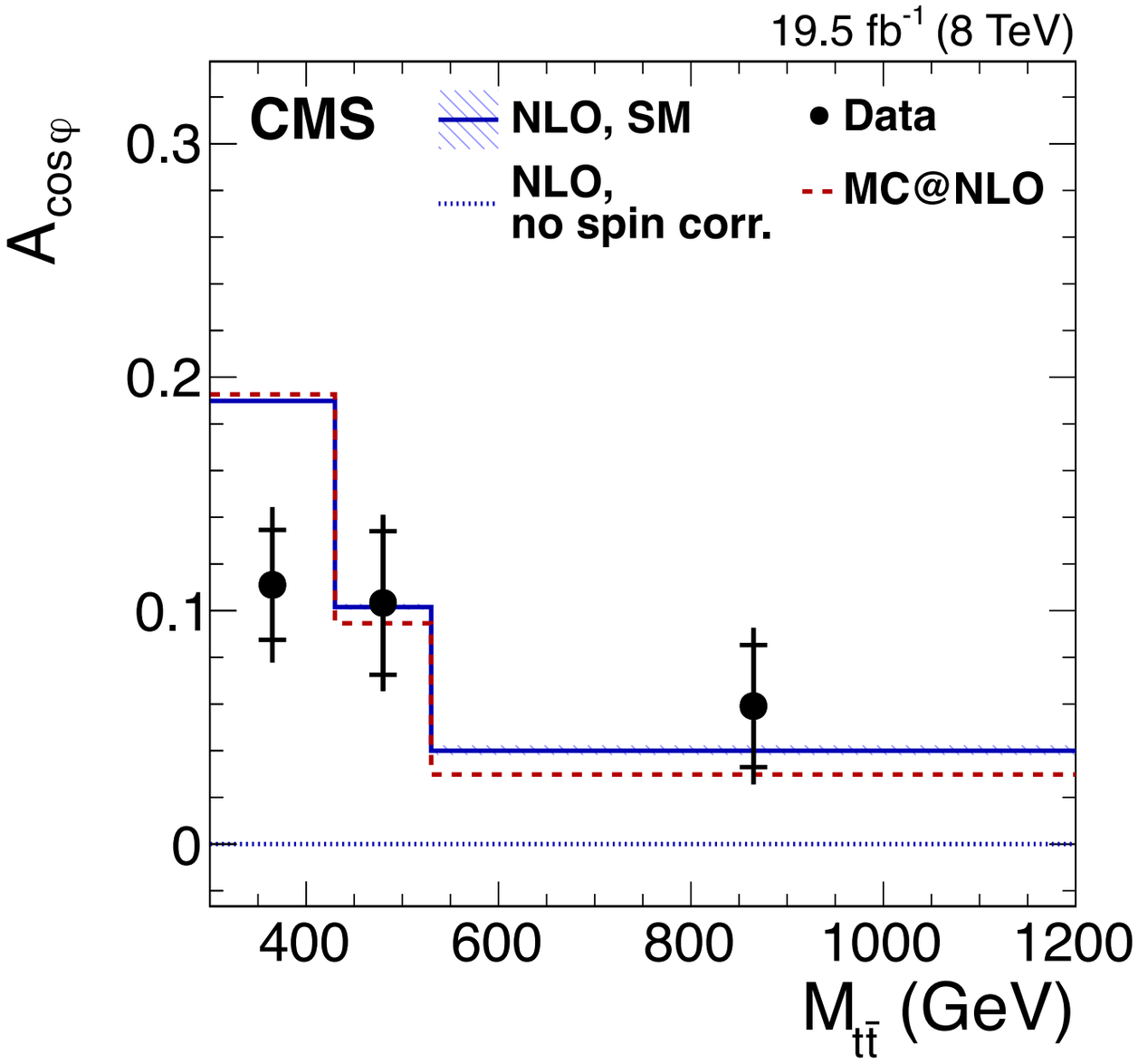

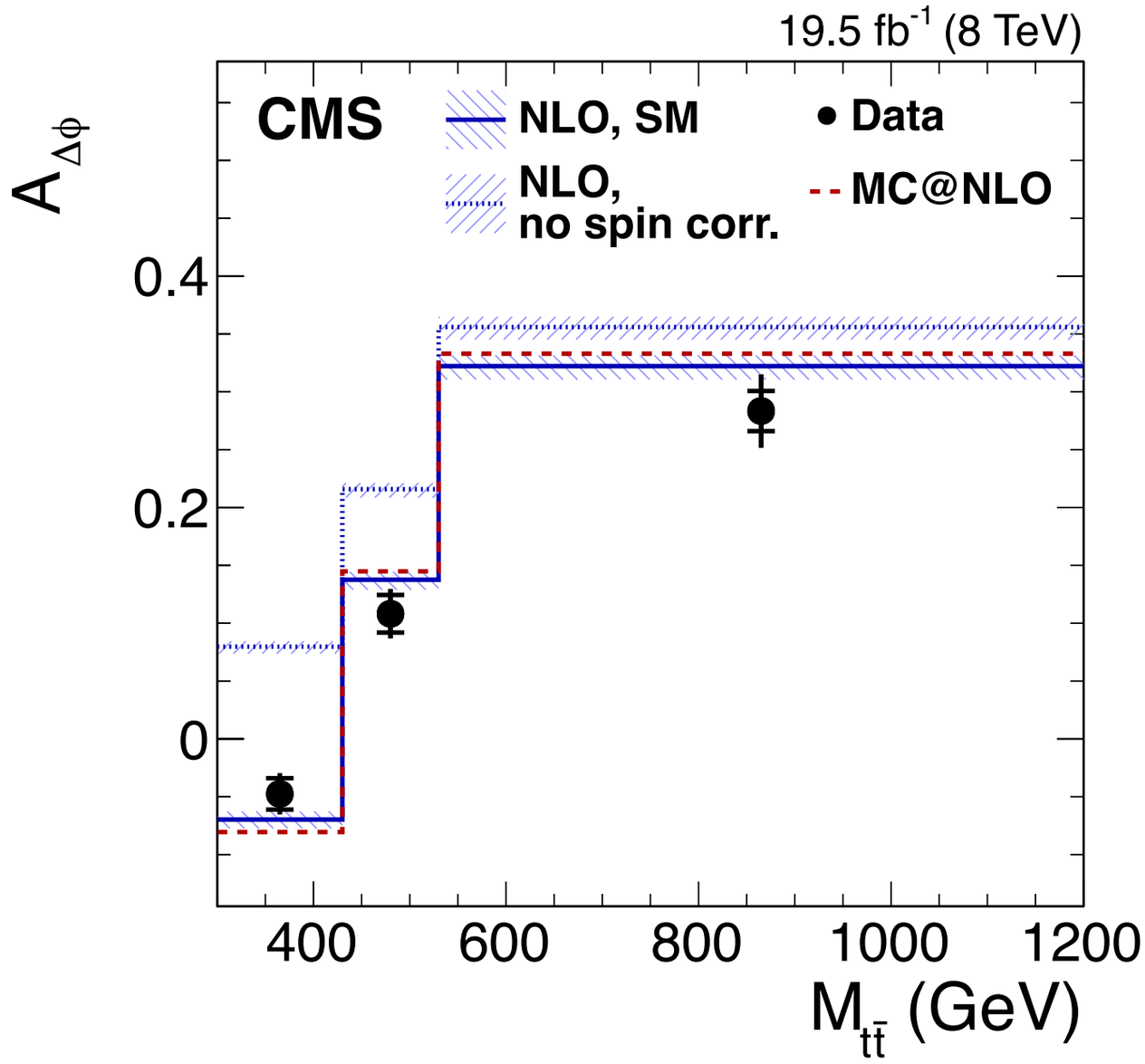

- SM spin correlations have most structure wrt $M_{t\bar{t}}$
- Measuring wrt $M_{t\bar{t}}$ **minimises the top p_T modelling systematic:**
  - **$f_{SM} = 1.12 \pm 0.06 \pm 0.08\,^{+0.08}_{-0.11}$, ~8σ from zero** (limited by NLO scale uncertainties!)

Probing SUSY with spin correlations

- For $\Delta m \sim m_t$, $\tilde{t}\tilde{t}^*$ events look similar to **uncorrelated** $t\bar{t}$ events
- But they have only ~1/6 of the cross section for $m_{\tilde{t}} = m_t$
  - our ~8σ sensitivity to spin correlations becomes ~1.3σ to stops !
- Total cross section measurement also sensitive to contribution from stops
  - combining the two, beginning to have sensitivity

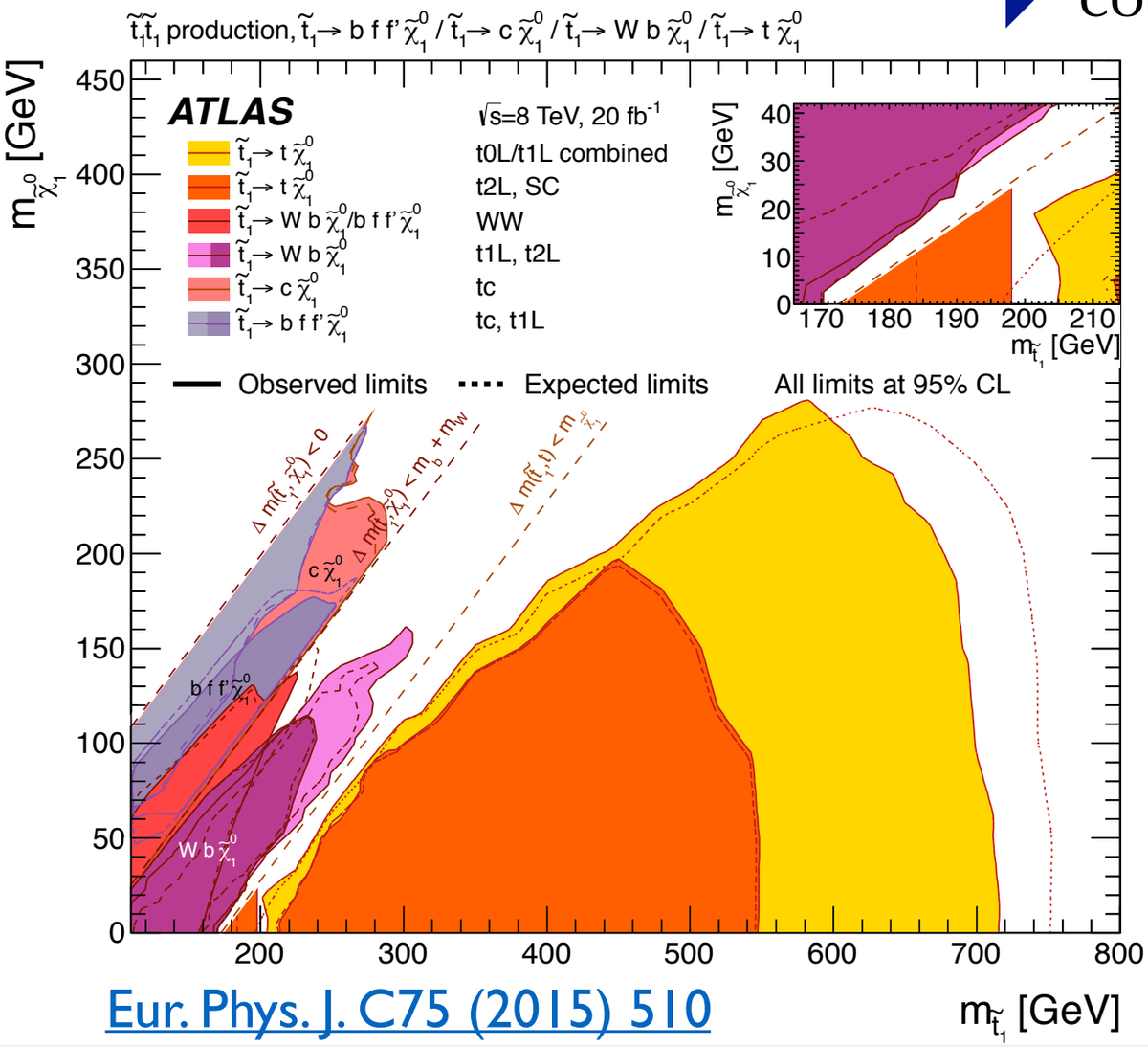

Eur. Phys. J. C75 (2015) 510

- ATLAS excludes
  $m_t < m_{stop} < 198$ GeV
  Phys. Rev. Lett. 114, 142001 (2015)
- CMS excludes
  $m_t < m_{stop} < 190$ GeV
  (using xsec alone)
  CMS-PAS-TOP-13-004

Important not to miss any naturally favoured region!

Bernreuther, Heisler & Si, 1508.05271

Table 1: Transformation properties of the structure functions defined in (2.6), (2.7) with respect to CP, P, and $\mathrm{T_N}$. The implications of Bose symmetry in the last column apply only to $I = gg$.

	CP	P	$\mathrm{T_N}$ (abs $\mathcal{T}=0$)	$\mathrm{CPT_N}$ (abs $\mathcal{T}=0$)	Bose symmetry
$A^I(y)$	$A^I(y)$	$A^I(y)$	$A^I(y)$	$A^I(y)$	$A^{gg}(-y)$
$b_r^{I\pm}(y)$	$b_r^{I\mp}(y)$	$-b_r^{I\pm}(y)$	$b_r^{I\pm}(y)$	$b_r^{I\mp}(y)$	$-b_r^{gg\pm}(-y)$
$b_k^{I\pm}(y)$	$b_k^{I\mp}(y)$	$-b_k^{I\pm}(y)$	$b_k^{I\pm}(y)$	$b_k^{I\mp}(y)$	$b_k^{gg\pm}(-y)$
$b_n^{I\pm}(y)$	$b_n^{I\mp}(y)$	$b_n^{I\pm}(y)$	$-b_n^{I\pm}(y)$	$-b_n^{I\mp}(y)$	$-b_n^{gg\pm}(-y)$
$c_{rr}^I(y)$	$c_{rr}^I(y)$	$c_{rr}^I(y)$	$c_{rr}^I(y)$	$c_{rr}^I(y)$	$c_{rr}^{gg}(-y)$
$c_{kk}^I(y)$	$c_{kk}^I(y)$	$c_{kk}^I(y)$	$c_{kk}^I(y)$	$c_{kk}^I(y)$	$c_{kk}^{gg}(-y)$
$c_{nn}^I(y)$	$c_{nn}^I(y)$	$c_{nn}^I(y)$	$c_{nn}^I(y)$	$c_{nn}^I(y)$	$c_{nn}^{gg}(-y)$
$c_{rk}^I(y)$	$c_{rk}^I(y)$	$c_{rk}^I(y)$	$c_{rk}^I(y)$	$c_{rk}^I(y)$	$-c_{rk}^{gg}(-y)$
$c_{rn}^I(y)$	$c_{rn}^I(y)$	$-c_{rn}^I(y)$	$-c_{rn}^I(y)$	$-c_{rn}^I(y)$	$c_{rn}^{gg}(-y)$
$c_{kn}^I(y)$	$c_{kn}^I(y)$	$-c_{kn}^I(y)$	$-c_{kn}^I(y)$	$-c_{kn}^I(y)$	$-c_{kn}^{gg}(-y)$
$c_r^I(y)$	$-c_r^I(y)$	$-c_r^I(y)$	$-c_r^I(y)$	$c_r^I(y)$	$-c_r^{gg}(-y)$
$c_k^I(y)$	$-c_k^I(y)$	$-c_k^I(y)$	$-c_k^I(y)$	$c_k^I(y)$	$c_k^{gg}(-y)$
$c_n^I(y)$	$-c_n^I(y)$	$c_n^I(y)$	$c_n^I(y)$	$-c_n^I(y)$	$-c_n^{gg}(-y)$

Table 6: The correlation coefficients of (4.8), respectively of (4.17), (4.18) and (4.19), and sums and differences for different choices of reference axes.

Correlation		sensitive to
$C(n,\,n)$	c_{nn}^{I}	P-, CP-even
$C(r,\,r)$	c_{rr}^{I}	P-, CP-even
$C(k,\,k)$	c_{kk}^{I}	P-, CP-even
$C(r,\,k)+C(k,\,r)$	c_{rk}^{I}	P-, CP-even
$C(n,\,r)+C(r,\,n)$	c_{rn}^{I}	P-odd, CP-even, absorptive
$C(n,\,k)+C(k,\,n)$	c_{kn}^{I}	P-odd, CP-even, absorptive
$C(r,\,k)-C(k,\,r)$	c_{n}^{I}	P-even, CP-odd, absorptive
$C(n,\,r)-C(r,\,n)$	c_{k}^{I}	P-odd, CP-odd
$C(n,\,k)-C(k,\,n)$	$-c_{r}^{I}$	P-odd, CP-odd
$B_1(n)+B_2(n)$	$b_{n}^{I+}+b_{n}^{I-}$	P-, CP-even, absorptive
$B_1(n)-B_2(n)$	$b_{n}^{I+}-b_{n}^{I-}$	P-even, CP-odd
$B_1(r)+B_2(r)$	$b_{r}^{I+}+b_{r}^{I-}$	P-odd, CP-even
$B_1(r)-B_2(r)$	$b_{r}^{I+}-b_{r}^{I-}$	P-odd, CP-odd, absorptive
$B_1(k)+B_2(k)$	$b_{k}^{I+}+b_{k}^{I-}$	P-odd,CP-even
$B_1(k)-B_2(k)$	$b_{k}^{I+}-b_{k}^{I-}$	P-odd, CP-odd, absorptive
$B_1(k^*)+B_2(k^*)$	$b_{k}^{I+}+b_{k}^{I-}$	P-odd,CP-even
$B_1(k^*)-B_2(k^*)$	$b_{k}^{I+}-b_{k}^{I-}$	P-odd, CP-odd, absorptive
$B_1(r^*)+B_2(r^*)$	$b_{r}^{I+}+b_{r}^{I-}$	P-odd, CP-even
$B_1(r^*)-B_2(r^*)$	$b_{r}^{I+}-b_{r}^{I-}$	P-odd, CP-odd, absorptive

Bernreuther, Heisler & Si, 1508.05271

Table 8: The correlation coefficients B at NLOW in the SM and the non-zero contributions of the dimensionless anomalous couplings defined in section 3. The central values correspond to the scales $\mu = m_t$. The uncertainties refer to $\mu = m_t/2$ and $\mu = 2m_t$.

–		NLOW	$\propto \hat{c}_{VA}$	$\propto \hat{c}_3$
$B_1(r) + B_2(r)$	8 TeV	$(2.9^{+1.9}_{-1.4}) \cdot 10^{-3}$	$0.298^{+0.014}_{-0.014}$	$(3.89^{+0.24}_{-0.23}) \cdot 10^{-2}$
	13 TeV	$(3.2^{+2.3}_{-1.7}) \cdot 10^{-3}$	$0.210^{+0.009}_{-0.009}$	$(2.55^{+0.14}_{-0.14}) \cdot 10^{-2}$
	14 TeV	$(3.3^{+2.3}_{-1.8}) \cdot 10^{-3}$	$0.199^{+0.008}_{-0.008}$	$(2.39^{+0.13}_{-0.13}) \cdot 10^{-2}$
$B_1(k) + B_2(k)$	8 TeV	$(6.1^{+2.3}_{-1.7}) \cdot 10^{-3}$	$2.100^{+0.081}_{-0.078}$	$0.283^{+0.015}_{-0.014}$
	13 TeV	$(8.0^{+3.4}_{-2.4}) \cdot 10^{-3}$	$1.607^{+0.051}_{-0.052}$	$0.201^{+0.009}_{-0.009}$
	14 TeV	$(8.3^{+3.5}_{-3.5}) \cdot 10^{-3}$	$1.542^{+0.047}_{-0.047}$	$0.191^{+0.008}_{-0.008}$
–		NLOW	$\propto \hat{c}_{AV}$	$\propto \hat{c}_1 - \hat{c}_2 + \hat{c}_3$
$B_1(r^*) + B_2(r^*)$	8 TeV	$< 10^{-3}$	$1.166^{+0.063}_{-0.060}$	$0.244^{+0.014}_{-0.014}$
	13 TeV	$< 10^{-3}$	$0.792^{+0.040}_{-0.039}$	$0.164^{+0.009}_{-0.009}$
	14 TeV	$< 10^{-3}$	$0.746^{+0.037}_{-0.036}$	$0.154^{+0.008}_{-0.008}$
$B_1(k^*) + B_2(k^*)$	8 TeV	$< 10^{-3}$	$1.204^{+0.054}_{-0.052}$	$0.251^{+0.013}_{-0.012}$
	13 TeV	$< 10^{-3}$	$0.883^{+0.034}_{-0.034}$	$0.183^{+0.008}_{-0.008}$
	14 TeV	$< 10^{-3}$	$0.842^{+0.032}_{-0.032}$	$0.174^{+0.007}_{-0.007}$
–		NLO QCD	EW	
$B_1(n) + B_2(n)$	8 TeV	$(6.93^{+0.84}_{-0.72}) \cdot 10^{-3}$	$(3.44^{+0.09}_{-0.07}) \cdot 10^{-3}$	
	13 TeV	$(7.45^{+0.90}_{-0.72}) \cdot 10^{-3}$	$(3.89^{+0.06}_{-0.06}) \cdot 10^{-3}$	
	14 TeV	$(7.52^{+0.90}_{-0.73}) \cdot 10^{-3}$	$(3.94^{+0.06}_{-0.05}) \cdot 10^{-3}$	
–		$\propto \hat{c}_{(-+)}$		
$B_1(n) - B_2(n)$	8 TeV	$4.148^{+0.115}_{-0.128}$		
	13 TeV	$4.876^{+0.108}_{-0.124}$		
	14 TeV	$4.975^{+0.109}_{-0.124}$		

Bernreuther, Heisler & Si, 1508.05271

Table 7: The correlation coefficients C at NLOW in the SM and the non-zero contributions of the dimensionless anomalous couplings defined in section 3. The central values correspond to the scales $\mu = m_t$. The uncertainties refer to $\mu = m_t/2$ and $\mu = 2m_t$.

–		NLOW	$\propto \hat{c}_{VV}$	$\propto \hat{c}_1$	$\propto \hat{\mu}_t$
$C(n,\, n)$	8 TeV	$0.332^{+0.002}_{-0.002}$	$-0.150^{+0.010}_{-0.012}$	$(-1.76^{+0.15}_{-0.17}) \cdot 10^{-2}$	$1.831^{+0.038}_{-0.036}$
	13 TeV	$0.326^{+0.002}_{-0.002}$	$(-7.99^{+0.80}_{-0.85}) \cdot 10^{-2}$	$(-8.21^{+0.99}_{-1.08}) \cdot 10^{-3}$	$2.025^{+0.025}_{-0.024}$
	14 TeV	$0.325^{+0.002}_{-0.002}$	$(-7.21^{+0.75}_{-0.81}) \cdot 10^{-2}$	$(-7.20^{+0.94}_{-0.99}) \cdot 10^{-3}$	$2.047^{+0.022}_{-0.022}$
$C(r,\, r)$	8 TeV	$0.055^{+0.009}_{-0.007}$	$-0.934^{+0.033}_{-0.037}$	$-0.122^{+0.006}_{-0.006}$	$2.313^{+0.032}_{-0.031}$
	13 TeV	$0.071^{+0.008}_{-0.006}$	$-0.697^{+0.027}_{-0.027}$	$(-8.46^{+0.41}_{-0.43}) \cdot 10^{-2}$	$2.475^{+0.020}_{-0.019}$
	14 TeV	$0.072^{+0.008}_{-0.006}$	$-0.665^{+0.025}_{-0.026}$	$(-7.99^{+0.39}_{-0.40}) \cdot 10^{-2}$	$2.493^{+0.019}_{-0.019}$
$C(k,\, k)$	8 TeV	$0.318^{+0.003}_{-0.002}$	$-1.570^{+0.049}_{-0.053}$	$-0.209^{+0.009}_{-0.010}$	$0.964^{+0.009}_{-0.009}$
	13 TeV	$0.331^{+0.002}_{-0.002}$	$-1.218^{+0.039}_{-0.040}$	$-0.151^{+0.007}_{-0.007}$	$0.917^{+0.006}_{-0.006}$
	14 TeV	$0.331^{+0.002}_{-0.002}$	$-1.169^{+0.037}_{-0.038}$	$-0.143^{+0.006}_{-0.006}$	$0.911^{+0.006}_{-0.005}$
$C(r,\, k) + C(k,\, r)$	8 TeV	$-0.226^{+0.004}_{-0.004}$	$-0.430^{+0.016}_{-0.018}$	$(-5.42^{+0.28}_{-0.30}) \cdot 10^{-2}$	$0.720^{+0.008}_{-0.010}$
	13 TeV	$-0.206^{+0.002}_{-0.002}$	$-0.306^{+0.014}_{-0.014}$	$(-3.58^{+0.20}_{-0.20}) \cdot 10^{-2}$	$0.740^{+0.001}_{-0.002}$
	14 TeV	$-0.204^{+0.004}_{-0.002}$	$-0.290^{+0.012}_{-0.012}$	$(-3.34^{+0.18}_{-0.20}) \cdot 10^{-2}$	$0.740^{+0.002}_{-0.004}$
–		NLOW			
$C(n,\, r) + C(r,\, n)$	8 TeV	$(1.03^{+0.01}_{-0.01}) \cdot 10^{-3}$			
	13 TeV	$(1.06^{+0.01}_{-0.01}) \cdot 10^{-3}$			
	14 TeV	$(1.07^{+0.01}_{-0.01}) \cdot 10^{-3}$			
$C(n,\, k) + C(k,\, n)$	8 TeV	$(2.32^{+0.01}_{-0.01}) \cdot 10^{-3}$			
	13 TeV	$(2.15^{+0.04}_{-.007}) \cdot 10^{-3}$			
	14 TeV	$(2.12^{+0.03}_{-0.08}) \cdot 10^{-3}$			
–		$\propto \hat{c}_{(--)}$	$\propto \hat{d}_t$		
$C(n,\, r) - C(r,\, n)$	8 TeV	$-1.321^{+0.021}_{-0.020}$	$-3.705^{+0.084}_{-0.087}$		
	13 TeV	$-1.226^{+0.007}_{-0.004}$	$-4.143^{+0.053}_{-0.056}$		
	14 TeV	$-1.217^{+0.005}_{-0.002}$	$-4.195^{+0.052}_{-0.052}$		
$C(n,\, k) - C(k,\, n)$	8 TeV	$-1.665^{+0.073}_{-0.058}$	$-0.721^{+0.021}_{-0.019}$		
	13 TeV	$-2.157^{+0.108}_{-0.087}$	$-0.800^{+0.006}_{-0.003}$		
	14 TeV	$-2.236^{+0.112}_{-0.091}$	$-0.805^{+0.004}_{-0.001}$		

C matrix in LO QCD

1. $q\bar{q} \to t\bar{t}$

Baumgart and Tweedie, 1212.4888

$$\text{off-diagonal basis}: \quad C = \begin{pmatrix} \frac{\beta^2 \sin^2\Theta}{2-\beta^2\sin^2\Theta} & 0 & 0 \\ 0 & \frac{-\beta^2\sin^2\Theta}{2-\beta^2\sin^2\Theta} & 0 \\ 0 & 0 & 1 \end{pmatrix}$$

$$\text{helicity basis}: \quad C = \begin{pmatrix} \frac{(2-\beta^2)\sin^2\Theta}{2-\beta^2\sin^2\Theta} & 0 & \frac{-\sin 2\Theta}{\gamma(2-\beta^2\sin^2\Theta)} \\ 0 & \frac{-\beta^2\sin^2\Theta}{2-\beta^2\sin^2\Theta} & 0 \\ \frac{-\sin 2\Theta}{\gamma(2-\beta^2\sin^2\Theta)} & 0 & \frac{2\cos^2\Theta+\beta^2\sin^2\Theta}{2-\beta^2\sin^2\Theta} \end{pmatrix}$$

2. $gg \to t\bar{t}$

helicity basis:

$$C = \begin{pmatrix} \frac{-1+\beta^2(2-\beta^2)(1+\sin^4\Theta)}{1+2\beta^2\sin^2\Theta-\beta^4(1+\sin^4\Theta)} & 0 & \frac{-\beta^2\sin 2\Theta\sin^2\Theta}{\gamma(1+2\beta^2\sin^2\Theta-\beta^4(1+\sin^4\Theta))} \\ 0 & \frac{-1+2\beta^2-\beta^4(1+\sin^4\Theta)}{1+2\beta^2\sin^2\Theta-\beta^4(1+\sin^4\Theta)} & 0 \\ \frac{-\beta^2\sin 2\Theta\sin^2\Theta}{1+2\beta^2\sin^2\Theta-\beta^4(1+\sin^4\Theta)} & 0 & \frac{-1+\beta^2\left(\beta^2(1+\sin^4\Theta)+(\sin^2 2\Theta)/2\right)}{1+2\beta^2\sin^2\Theta-\beta^4(1+\sin^4\Theta)} \end{pmatrix}$$